



HAL
open science

Experimental investigations of buckling behaviour of steel scaffolds

C. Mercier, Abdelouahab Khelil, Firas Al-Mahmoud, J.-L. Blin-Lacroix, A. Pamies

► **To cite this version:**

C. Mercier, Abdelouahab Khelil, Firas Al-Mahmoud, J.-L. Blin-Lacroix, A. Pamies. Experimental investigations of buckling behaviour of steel scaffolds. *Structures*, 2021, 33, pp.433-450. 10.1016/j.istruc.2021.04.045 . hal-03219864

HAL Id: hal-03219864

<https://hal.univ-lorraine.fr/hal-03219864v1>

Submitted on 9 May 2023

HAL is a multi-disciplinary open access archive for the deposit and dissemination of scientific research documents, whether they are published or not. The documents may come from teaching and research institutions in France or abroad, or from public or private research centers.

L'archive ouverte pluridisciplinaire **HAL**, est destinée au dépôt et à la diffusion de documents scientifiques de niveau recherche, publiés ou non, émanant des établissements d'enseignement et de recherche français ou étrangers, des laboratoires publics ou privés.



Distributed under a Creative Commons Attribution - NonCommercial 4.0 International License

EXPERIMENTAL INVESTIGATIONS OF BUCKLING BEHAVIOUR OF STEEL SCAFFOLDS

C. Mercier¹, A. Khelil¹, F. Al Mahmoud¹, J.-L. Blin-Lacroix¹, A. Pamies²

¹University of Lorraine, IJL, UMR CNRS 7198, Nancy France
charlotte.mercier@univ-lorraine.fr, abdelouahab.khelil@univ-lorraine.fr, firas.al-mahmoud@univ-lorraine.fr, jean-luc.blin-lacroix@univ-lorraine.fr,

²SFECE, Paris
alain.pamies11@orange.fr

Abstract. The analysis and design of structures sensitive to second order effects require the consideration of initial imperfections. Scaffold structures, due to their low stiffness, are very sensitive to second order effects. The accuracy of the design of these structures relies in part on the estimation of initial imperfections affecting the structure. In the 1960s, the C.E.C.M., the European Convention of Steel Construction, carried out a series of experimental tests to determine the degree of initial imperfections of each type of cross-section. Five buckling curves were established. The European design code for steel structures, Eurocode 3 Part 1-1, classifies hot-rolled hollow tubular sections as profiles with few imperfections, i.e. buckling curve 'a', and cold-formed sections as sections with many imperfections, i.e. buckling curve 'c'. A test campaign was conducted to analyse the experimental buckling behaviour of hot-rolled and cold-formed hollow sections of scaffold structures. Twenty-nine buckling tests on simply supported members and nine buckling tests on scaffolding ladders, from various European suppliers, were carried out. Statistical studies of the experimental results point out that the estimate of the initial imperfection currently defined for the hot-rolled and cold-formed tubular sections is far too penalizing for sections used in scaffolding.

Keywords: Scaffold, Buckling behaviour, Buckling curve, Initial imperfections, Circular tubular section

1 Introduction

The scaffold structures present a low rigidity, with regard to those of buildings, and a high slenderness ratio. Under axial compression, cross-section resistance does not govern the behaviour of such structures. Indeed, second order effects appear and the failure of these structures is caused by divergence of equilibrium (Figure 1). Amplitude of these second order effects is influenced by the presence of initial imperfections. It is therefore necessary to include them in the structures' design.

The structures design is performed in two steps: (i) the structures' analysis, known as the global analysis; (ii) the resistance and stability verifications. The more the global analysis is carried out in depth, the more verification criteria, which result from it, are simple, and *vice versa*.

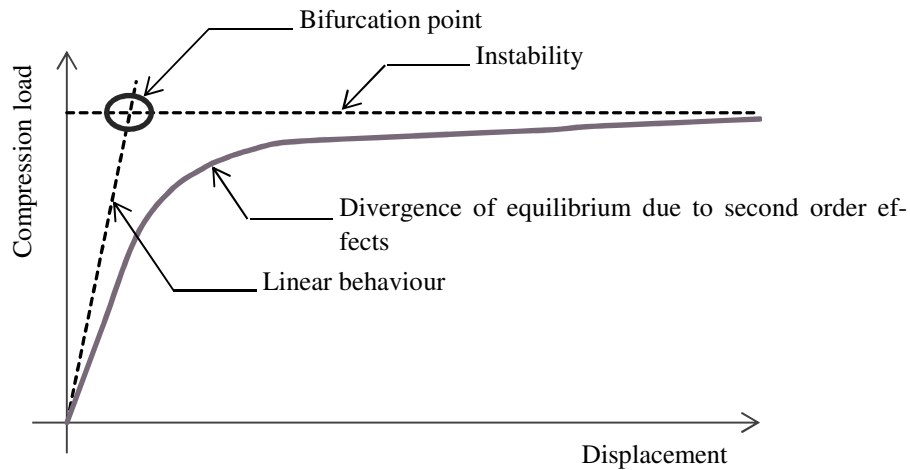


Figure 1 Behaviour of column under axial compression

The European design code for steel structures, Eurocode 3 Part 1-1 [1], allow to take them into account in two different ways:

- The global analysis includes initial imperfections and second order effects. The structures verification is therefore based on cross-section criteria.
- The global analysis does not include initial imperfections and second order effects. The structures verification is therefore done using so-called instability criteria.

However, whatever the method used, the precision of the verification relies on the assessment of the initial imperfections affecting the structures. Indeed, if the initial imperfections of a structure are overestimated, the internal stresses will in turn be overestimated; this will lead to the oversizing of the structure and therefore an additional cost for the manufacturers. On the contrary, if the initial imperfections are underestimated, the internal stresses will also be underestimated and the structure will be undersized, which will lead to safety problems. An accurate estimation of the initial imperfections affecting scaffolding structures is therefore crucial for the optimal design of these structures.

In the 1960s, the European Convention of Steel Construction (C.E.C.M.) [2] led a test campaign to assess the degree of initial imperfections in each type of cross-section. This led, in Eurocode 3 Part 1-1, to the creation of five buckling curves, from 'a₀' to 'd', corresponding to almost perfect profiles to profiles with a significant degree of initial imperfection, respectively. Each of these buckling curves corresponds to an imperfection factor α , enabling to take into account the degree of initial imperfections in the structure design. Steel scaffold structures are mostly designed in cold-formed tubular sections, but can equally be made with hot-rolled sections. The imperfection factor is therefore set at 0.49 in the first case and 0.21 in the second.

Scaffolding structures have initial imperfections that affect the stability and load-bearing capacity of the structure. The study of the stability of scaffolds has been the subject of many researches over the last fifty years, because of the risk of collapse. Milojkovic *et al.* [3,4] presented a report on an investigation conducted by the Health and Safety Executive [5] in the United Kingdom into inherent defects in scaffold structures. They showed that these defects can reduce the capacity of a scaffold to less than 10% of its design capacity. Among the defects, they identified lack of anchorage to the façade, verticality defects of the structure, straightness defects of the scaffold standards and inadequate foundations. On the other hand, Lew [6] showed that errors in falsework design are also one of the main sources of scaffold collapses. Many researchers have thus devoted themselves to the study of the stability of scaffolds and to the development of structural models allowing their load capacities to be estimated.

Peng *et al.* [7] carried out experimental studies to determine the influence on the load capacity of

heavy duty scaffolds of different parameters such as: (i) the different numbers of stories, (ii) the presence or absence of top and base screw jacks, (iii) the presence or absence of horizontal braces. They showed that the number of stories did not significantly reduce the load capacity of a scaffold. They also showed that the clevises and screw jack feet enhance the load capacity of a scaffold because they provide bending moment stiffness. The tests on scaffolds without horizontal braces showed that the horizontal braces provided strength to the structure.

Chandrangsu and Rasmussen [8,9] developed three-dimensional analysis models to predict the ultimate load of scaffold structures. The results obtained with the numerical model are compared with the results of a full-scale test carried out on a three-by-three bay formwork system, to ensure the reliability of the numerical model. They thus showed that the ultimate load from the numerical analysis is close to the failure loads obtained with the experimental test.

Peng *et al.* [10,11] examined the behaviour of two-storey steel scaffolds. They developed simplified theoretical analysis models in two-dimensional to predict the load capacity of scaffold structures. They showed [12] that a three-dimensional scaffold with regular configuration could be analysed more simply as a two-dimensional scaffold while being accurate and safe. Indeed, the cross-braces provide stiff lateral support in the three-dimensional scaffold.

Cimellaro and Domaneschi [13] investigated diverse type of steel scaffolds, namely: (i) joint tube scaffold, (ii) multidirectional scaffold and (iii) prefabricated scaffold. Finite element models are developed to identify the parameters that affect the load capacity of the scaffolds. They therefore showed that the presence of manufacturing imperfections, the eccentricities of the applied vertical load reduce the load capacity of the structure. They proposed an empirical formula to predict the critical load of common scaffolds.

Weesner and Jones [14] compared the load capacities of four different scaffolds obtained with experimental tests and finite element model. They concluded that numerical models provided a fair estimate of the load capacity of the scaffolds.

Peng and al. [15] studied the failure modes and load capacities of different scaffolds. Numerical analysis models supplemented these experimental tests. These models were initially calibrated using experimental tests. They were then used to deduce the load capacity of scaffolds with other conditions like additional diagonal bracings.

Klasson and al. [16] studied the effects of initial imperfections on the predicted strength and stiffness of steel columns. They highlighted the difficulty of studying complex structures containing several columns with multiple bracings. This difficulty stems from the considerable number of possible combinations in the shape of the initial imperfections.

Based on a review of the extant literature, many researches have been conducted to study the stability of the scaffolds. Cai *et al.* [17], Gao *et al.* [18], Iu [19], Chan and Lo [20], Liu *et al.* [21], Mercier *et al.* [22,23] and Yang *et al.* [24] agree that initial imperfections must be taken into account in the design of structures.

Zhao and Chen [25] developed numerical models to reveal the influence of the initial imperfections on scaffolding structures from one-bay to four-bay. They were therefore able to show that for an initial imperfection lower than $h/1000$, where h is the height of the scaffold modular, the ultimate load of capacity of the structure is merely slightly reduced. However, no real experimentation has been carried out to thoroughly determine the initial imperfections affecting the scaffold structures.

Gao *et al.* [18] conducted an experimental study on ten long steel columns with box-sections. They were therefore able to point out that the behaviour of this type of long column is similar to the curve 'b' in Eurocode 3.

In this article, similar experimental tests have been carried out to analyse the scaffold structures

behaviour under axial compression. Simply supported members and scaffold ladders, with a tubular section, were tested. The objective is to determine which buckling curve currently defined in Eurocode 3 better reflects the real behaviour of this type of structure. This test campaign was realized in collaboration with the French Syndicate of Scaffolding, Formwork and Shoring (SFECE).

2 Experimental tests on simply supported members

2.1 Experimental procedure

Tests on simply supported members [26] constitute the first step of the test campaign led in the laboratory to analyse the buckling behaviour of hollow tubular section structures. The test device (Figure 2) enabled to test simply supported members of 2 meters length. Simple steel tubes or steel scaffold standards were tested up to failure under axial compression. A total of ten hot-rolled members and nineteen cold-formed elements were tested.



Figure 2 Simply supported members test device

The tested members were galvanized and non-galvanized steel tubes, of 48.3 mm of diameter and 2.7 mm or 3.2 mm in thickness, widely used in the domain of scaffolding. The specific yielding strength and the modulus of elasticity were 320 MPa and 210 GPa, respectively. A naming system was assumed in the study to distinguish the tested specimens: TN for the non-galvanized tubes, TG for the galvanized tubes, PGD for the non-galvanized standards and PG for the galvanized standards.

Screwdrivers supports fabricated in the laboratory were the supports of the tested elements to ensure pin-jointed supports (Figure 3). The loading frame applied a vertical load on the specimens. A sensor displacement, located at mid-height of the tested element (Figure 4) and connected to the central processing unit, measured the lateral displacement of the element and acquire the data. It enabled monitoring the deflection of the single member according to the axial load. The experimental load-deflection responses were therefore obtained.



Figure 3 Screwdrivers supports

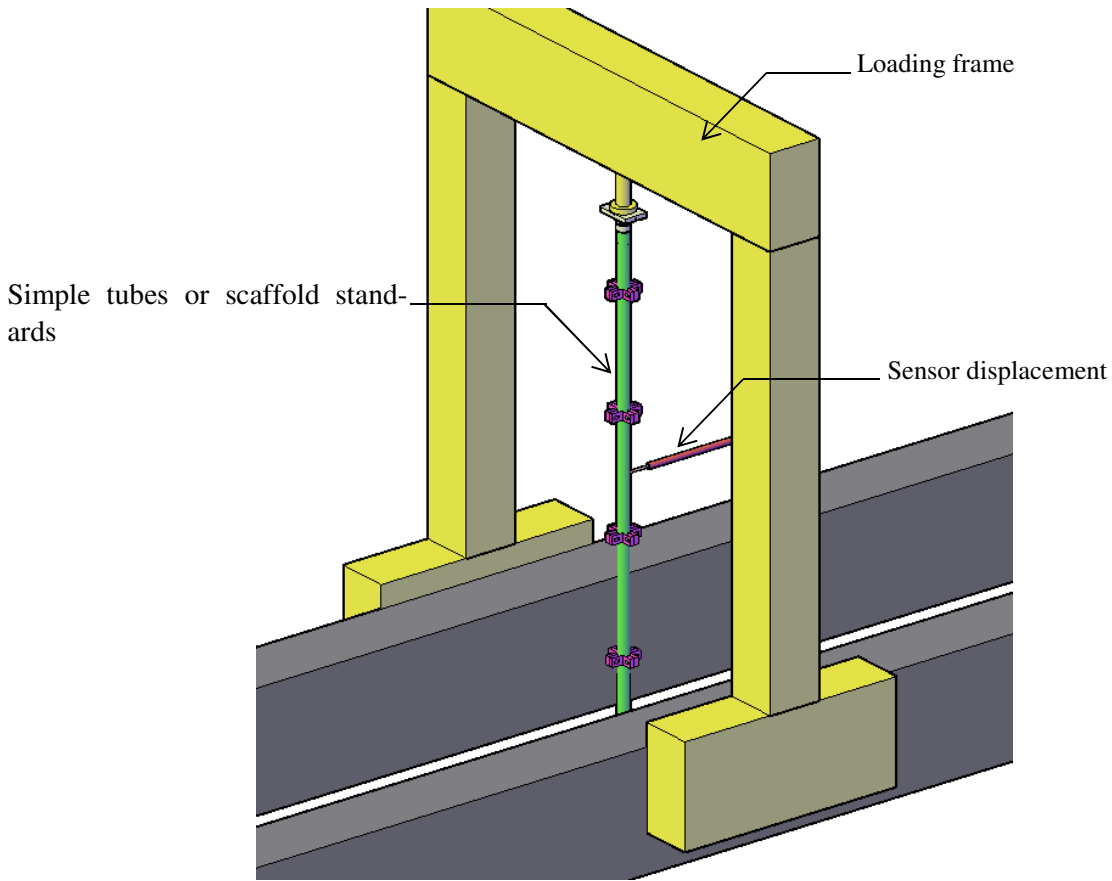


Figure 4 Configuration of the experimental test device for simply supported elements

2.2 Experimentations on hot-rolled hollow tubular sections

2.2.1 Test results

Figure 5 and Figure 6 illustrate the experimental load-deflection responses obtained from the acquisition of the measurements on hot-rolled simply supported elements.

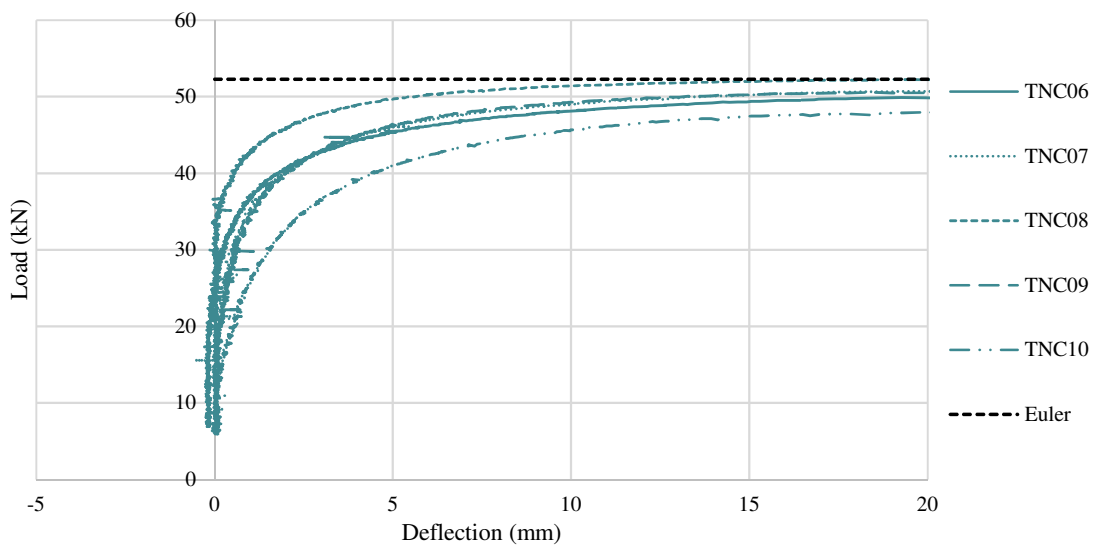


Figure 5 Experimental load-deflection responses at mid-height of the 2.7 mm of thickness hot-rolled elements

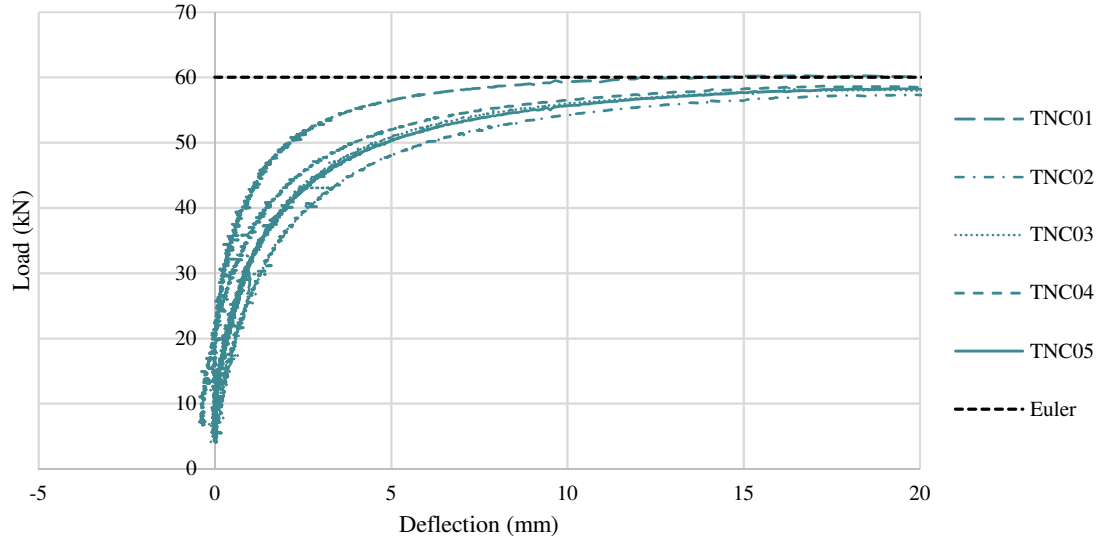


Figure 6 Experimental load-deflection responses at mid-height of the 3.2 mm of thickness hot-rolled elements. The experimental load and failure stress, of each tested specimen, are summarized in Table 1.

Table 1 Experimental load and failure stress on hot-rolled hollow tubular specimens

Section	Specimen	$P_{r,exp}$ (kN)	$\sigma_{r,exp}$ (MPa)
48.3 x 2.7 mm	TNC06	50	129.268
	TNC07	50.7	131.078
	TNC08	52.3	135.214
	TNC09	50.5	130.561
	TNC10	48	124.097
48.3 x 3.2 mm	TNC01	60.2	132.776
	TNC02	57.2	126.159
	TNC03	58	127.924
	TNC04	58.5	129.027
	TNC05	58.3	128.586

2.2.2 Statistical study

As part of the test campaign led by the C.E.C.M. in the 1960s, Jacquet [27] carried out a statistical study to determine conventional values of failure load and failure stress for each type of cross-section and each slenderness ratio tested. All these values of failure stress enable to draw up the current five buckling curves.

To enable the comparison between our experimental results and the results obtained in the 1960s, the statistical study carried out here is based on that of Jacquet's one.

To carry out the statistical study, it is necessary to ensure the distribution of the results can be approximated by a statistical normal distribution (Gauss distribution). The method of the moments was therefore employed.

The parameters determined with the method of the moments are the following:

$$(1) \text{ average: } m = \frac{\sum x}{N} \quad (1)$$

$$(2) \text{ deviation from the average: } y_i = x_i - m \quad (2)$$

$$(3) \text{ values: } S_2 = \sum y_i^2 \quad (3)$$

$$S_3 = \sum y_i^3 \quad (4)$$

$$S_4 = \sum y_i^4 \quad (5)$$

$$(4) \text{ values: } K_2 = \frac{S_2}{N-1} \quad (6)$$

$$K_3 = \frac{NS_3}{(N-1)(N-2)} \quad (7)$$

$$K_4 = \frac{N(N+1)S_4 - 3(N-1)S_3^2}{(N-1)(N-2)(N-3)} \quad (8)$$

$$(5) \text{ mean square deviation: } s = (K_2)^{1/2} \quad (9)$$

$$(6) \text{ values: } G_1 = \frac{K_3}{K_2^{3/2}} \quad (10)$$

$$G_2 = \frac{K_4}{K_2^2} \quad (11)$$

$$(7) \text{ mean square deviation } s_1 \text{ and } s_2: s_1 = \sqrt{\frac{6N(N-1)}{(N-2)(N+1)(N+3)}} \quad (12)$$

$$s_2 = \sqrt{\frac{24N(N-1)^2}{(N-3)(N-2)(N+3)(N+5)}} \quad (13)$$

$$(8) \text{ ratio: } V_1 = G_1/s_1 \quad (14)$$

$$V_2 = G_2/s_2 \quad (15)$$

A distribution is perfectly normal if $V_1 = V_2 = 0$. However, the normality of the distribution can be accepted as long as the values V_1 and V_2 remain low, i.e. less than 3. The values of V_1 and V_2 , given by Table 2, show that the distribution of the results can be considered as normal distribution.

Table 2 Parameters of the method of the moments for tests on simply supported hot-rolled members

Section	N	m (MPa)	s (MPa)	V_1	V_2
48.3 x 3.2 mm	5	128.894	2.245	0.485	0.541
48.3 x 2.7 mm	5	130.044	3.611	-0.303	0.246

The convention value of the failure stress is therefore done by the following equation:

$$\sigma_{u,conv} = m - 2s \quad (16)$$

Table 3 presents the conventional values of the failure load and the failure stress obtained from the experimental tests.

Table 3 Conventional values of the failure stress and the failure load for tests on simply supported hot-rolled members

Section	$\sigma_{u,conv}$ (MPa)	$P_{u,conv}$ (kN)	$\bar{\sigma} = \frac{\sigma_{u,conv}}{f_y}$
48.3 x 3.2 mm	124.404	56.404	0.518
48.3 x 2.7 mm	122.822	47.507	0.512

Figure 7 plots the distribution of experimental results. The conventional value of the failure stress is emphasised. It can be observed that the totality of the experimental results obtained is beyond the conventional failure stress resulting from the statistical study. Eurocode [28] states the 5% fractile value as the characteristic value, for an unfavourable low value. The both conventional values of the

failure stress are therefore safe.

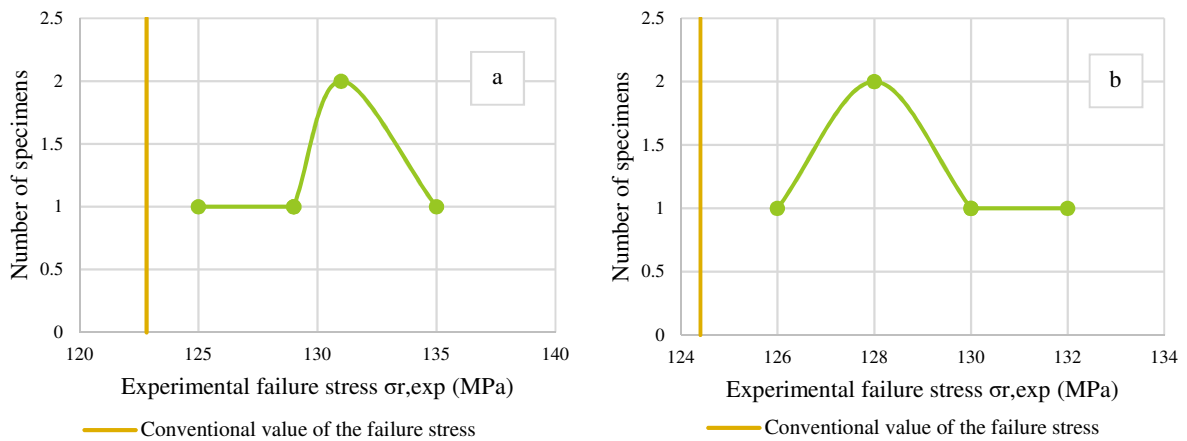


Figure 7 Distribution of experimental results for hot-rolled specimens: a) 48.3x2.7mm; b) 48.3x3.2mm

The conventional values of failure stress can be visualized among the European buckling curves (Figure 8). The reference buckling curve of such sections is the buckling curve 'a'.

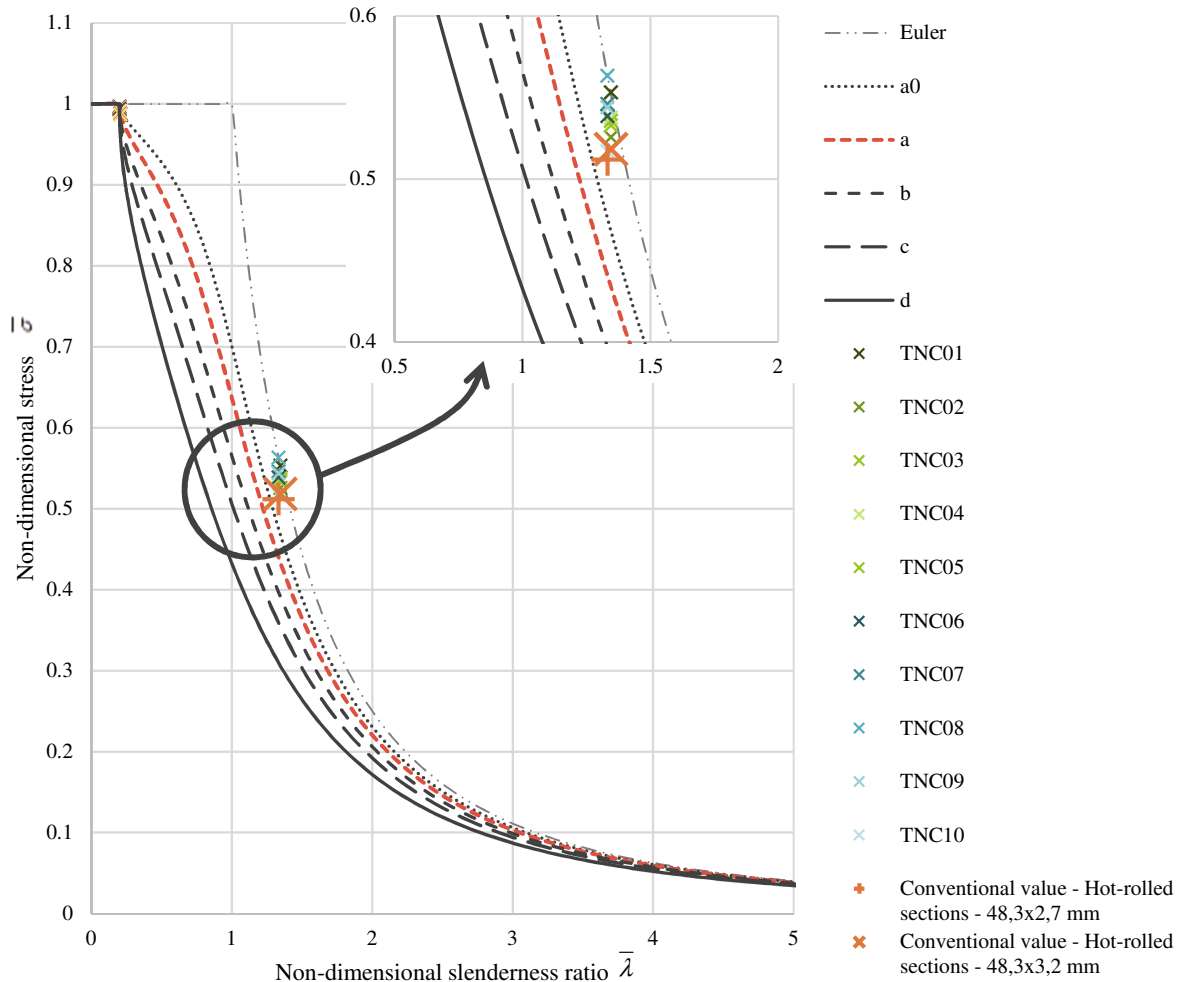


Figure 8 Comparison between experimental values and European buckling curves for hot-rolled elements

From the equation of the European buckling curves (equation (17)), drawn up by Maquoi and Rondal [29], the values of imperfection factor α stemming from the experiment were determined (Table 8).

$$\bar{\sigma} = \frac{1}{2\bar{\lambda}^2} \cdot \left(1 + \alpha\sqrt{\bar{\lambda}^2 - 0,04} + \bar{\lambda}^2 - \sqrt{\left(1 + \alpha\sqrt{\bar{\lambda}^2 - 0,04} + \bar{\lambda}^2 \right)^2 - 4\bar{\lambda}^2} \right) \quad (17)$$

Table 4 Experimental values of the imperfection factor for simply supported hot-rolled members

Section	α
48.3 x 3.2 mm	0.042
48.3 x 2.7 mm	0.066

It is apparent that the standard theoretical imperfection factor of Eurocode 3 is nowhere near the test results with respect to the hot-rolled elements. The imperfection factors determined from the statistical studies of the experimental test were around 0.05. Based on these results, it is possible to admit an imperfection factor of 0.13 would allow a better estimation of the initial imperfections affecting this type of element. This value of 0.13 could be applied to hot-rolled circular tubular steel sections, whose diameter and slenderness range are those common in the scaffold field.

2.2.3 Calibration of an analytical model and a finite element model

Two models have been developed: an analytical one and a finite element model.

For the analytical model, the mid-height deflection of the column must be expressed as a function of the load applied to the column. The deflection Δ physically measured at mid-height of the single member is:

$$\Delta = d_{fin} - e_0 = e_0 \cdot \frac{N}{N_{cr} - N} \quad (18)$$

where: d_{fin} represent the total deflection of the member under axial load, e_0 is the initial imperfection of the element, N is the compression load and N_{cr} is the critical load.

The article 5.3.2(11) of Eurocode 3 Part1-1 defines the initial imperfection e_0 as:

$$e_0 = \alpha \cdot (\bar{\lambda} - 0,2) \cdot \frac{W_{el}}{A} \quad (19)$$

where: α is the imperfection factor, $\bar{\lambda}$ is the non-dimensional slenderness, W_{el} is the elastic section modulus and A is the area of the cross-section.

The critical load is deduced from the equation:

$$N_{cr} = \frac{\pi^2 EI}{L_{cr}^2} \quad (20)$$

where L_{cr} is the buckling length of the element, E is the elastic modulus and I is the second moment of area.

The tested elements were single members with pin-jointed supports; therefore, the buckling length equals the length of the elements.

Equations (18) to (20) hence make it possible to establish the force-deflection response of a simply supported element for any value of imperfection factor α , i.e. several amplitudes of initial imperfections. It will thus be possible to compare the experimental response to different analytical responses, to obtain the analytical model that best reflects the actual behaviour of the structure. Three imperfection factor values will be compared:

- (i) an imperfection factor of 0.21: the conventional value for this type of cross-section established by Eurocode 3;

- (ii) an imperfection factor of 0.13: the imperfection factor value as close as possible to the values obtained by the statistical study;
- (iii) an imperfection factor value obtained through the calibration of the analytical model.

The second model developed is a finite element model. The software suite for finite element analysis Abaqus was used to create this finite element model. The measured dimensions of the components were used for cross-sectional properties in the finite element models. The nonlinearity properties of the steel material are applied to the model. The stress-strain relationship is based on results of tensile tests carried out on specimens from tested hot-rolled elements.

The calibration was achieved by changing the amplitude of the initial imperfections of the model, to obtain the finite element model that best reflects the actual behaviour of the structure. The failure (ultimate load) in the finite element model was observed when the load limit point was reached, which was associated with large displacements.

Figure 9 and Figure 10 compare finite element analysis results and analytical analysis results with the experimental load-deflection responses at mid-height of hot-rolled simply supported elements.

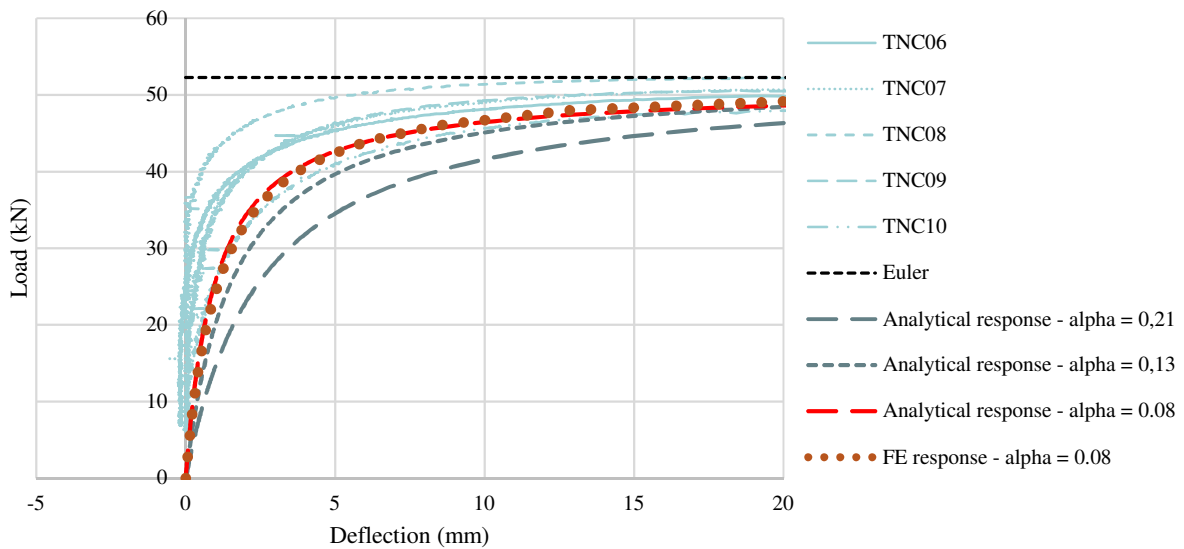


Figure 9 Calibration of load-deflection responses at mid-height of the 2.7 mm of thickness hot-rolled elements

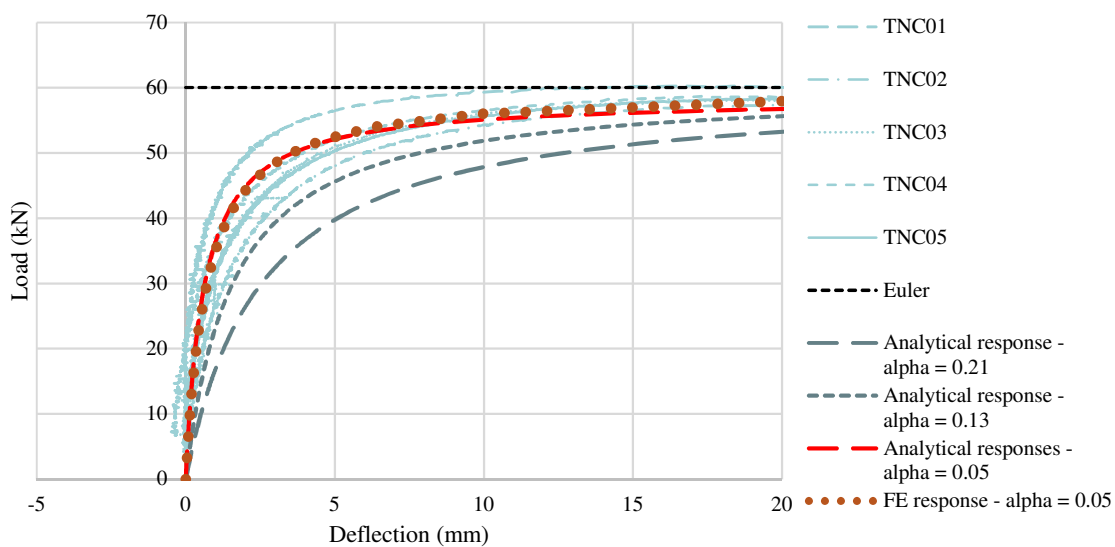


Figure 10 Calibration of load-deflection responses at mid-height of the 3.2 mm of thickness hot-rolled elements

The calibration results show that an imperfection factor of 0.08 and 0.05, for 2.7 mm and 3.7 mm of thickness respectively, gives a load-deflection response similar to the experimental one. These two imperfection factor values, derived from the analytical and finite element models, are significantly close to the values derived from the statistical study of the experimental results. The comparison of the load-deflection responses obtained with the analytical model and the finite element model shows that these two models are equivalent and both accurately predicting the behaviour and failure load of hot-rolled simply supported members.

The comparison of the analytical response with an imperfection factor of 0.21 to the experimental results makes it possible to affirm this response does not reflect the real behaviour of the structure. This implies that the initial imperfection degree of a buckling curve ‘a’, i.e. an imperfection factor of 0.21, is too important. The initial imperfections affecting these elements are actually considerably slighter, as experimentation has shown. An imperfection factor of 0.13, i.e. a buckling curve ‘a₀’, would make it possible to get closer to the experimental response while nevertheless preserving a safety margin.

2.3 Experimentations on cold-formed hollow tubular sections

2.3.1 Test results

Figure 11 and Figure 12 illustrate the experimental load-deflection responses obtained from the acquisition of the measurements on hot-rolled simply supported elements.

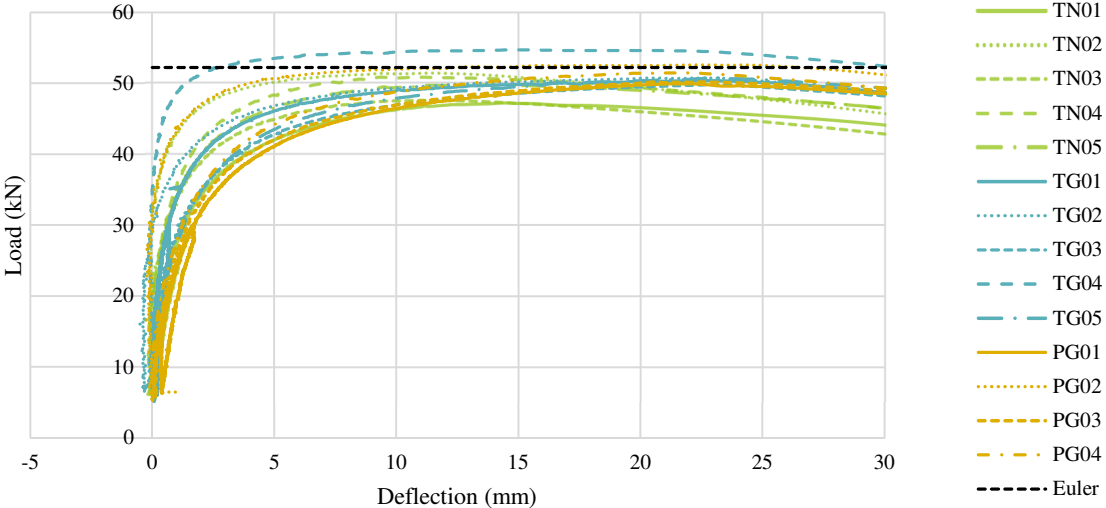


Figure 11 Experimental load-deflection responses at mid-height of the 2.7 mm of thickness cold-formed elements

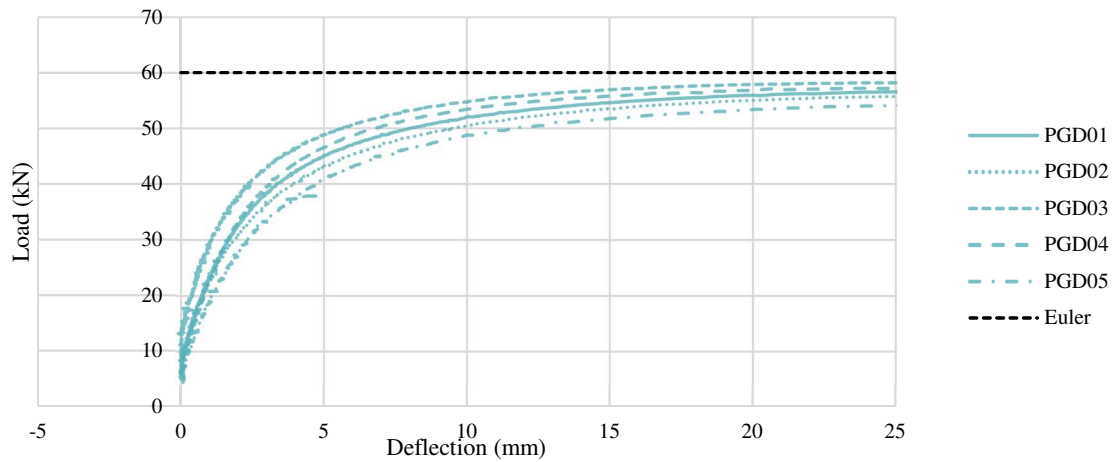


Figure 12 Experimental load-deflection responses at mid-height of the 3.2 mm of thickness cold-formed elements

The experimental load and failure stress, of each tested specimen, are summarized in Table 5.

Table 5 Experimental load and failure stress on cold-formed hollow tubular specimens

Section	Specimen	$P_{r,exp}$ (kN)	$\sigma_{r,exp}$ (MPa)
48.3 x 2.7 mm	TN01	47	121.512
	TN02	51.4	132.888
	TN03	47.5	122.805
	TN04	51	131.854
	TN05	49.8	128.751
	TG01	50.2	129.785
	TG02	50.7	131.078
	TG03	49.8	128.751
	TG04	54.7	141.419
	TG05	50.7	131.078
	PG01	50	129.268
	PG02	52.7	136.249
	PG03	50.1	129.527
	PG04	51.3	132.629
48.3 x 3.2 mm	PGD01	56.5	124.615
	PGD02	55.7	122.851
	PGD03	58.2	128.365
	PGD04	57	125.718
	PGD05	54.2	119.543

2.3.2 Statistical study

The statistical study is carried out on the similar principle as the previous one. Table 6 presents the values of V_1 and V_2 . In view of the values of the both parameters, it is therefore satisfactory to assume the normality of the distribution of the experimental results.

Table 6 Parameters of the method of the moments for tests on simply supported cold-formed members

Section	N	m (MPa)	s (MPa)	V_1	V_2
48.3 x 3.2 mm	5	124.219	3.611	-0.303	0.246
48.3 x 2.7 mm	14	130.542	4.868	0.301	0.123

The convention value of the failure stress is therefore done by the equation (16). Table 7 provides the conventional values of the failure load and the failure stress obtained from the experimental tests.

Table 7 Conventional values of the failure stress and the failure load for tests on simply supported members

Section	$\sigma_{u,conv}$ (MPa)	$P_{u,conv}$ (kN)	$\bar{\sigma} = \frac{\sigma_{u,conv}}{f_y}$
48.3 x 3.2 mm	116.978	53.037	0.366
48.3 x 2.7 mm	120.807	46.727	0.378

Figure 13 plots the distribution of experimental results. The conventional value of the failure stress is emphasised. As previously, it can be observed that the totality of the experimental results obtained is beyond the conventional failure stress resulting from the statistical study. The both conventional values of the failure stress are therefore safe with regard to the Eurocode [28] specifications.

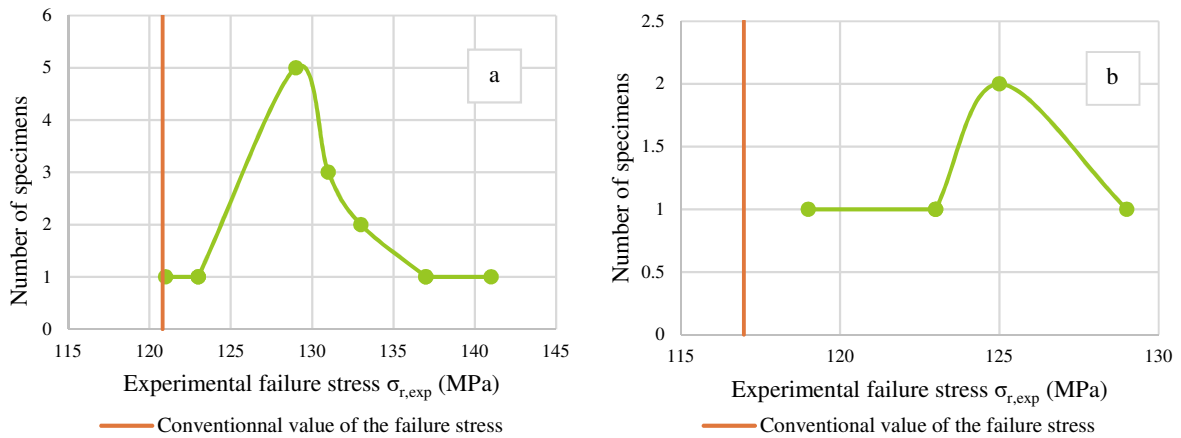
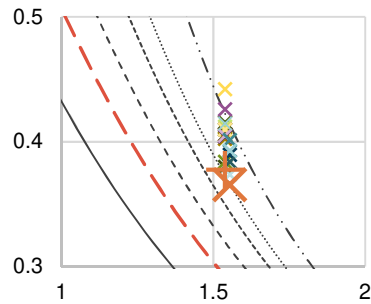


Figure 13 Distribution of experimental results for cold-formed specimens: a) 48.3x2.7mm; b) 48.3x3.2mm

The conventional values of failure stress can be visualized among the European buckling curves (Figure 14). The reference buckling curve of such sections is the buckling curve ‘c’.



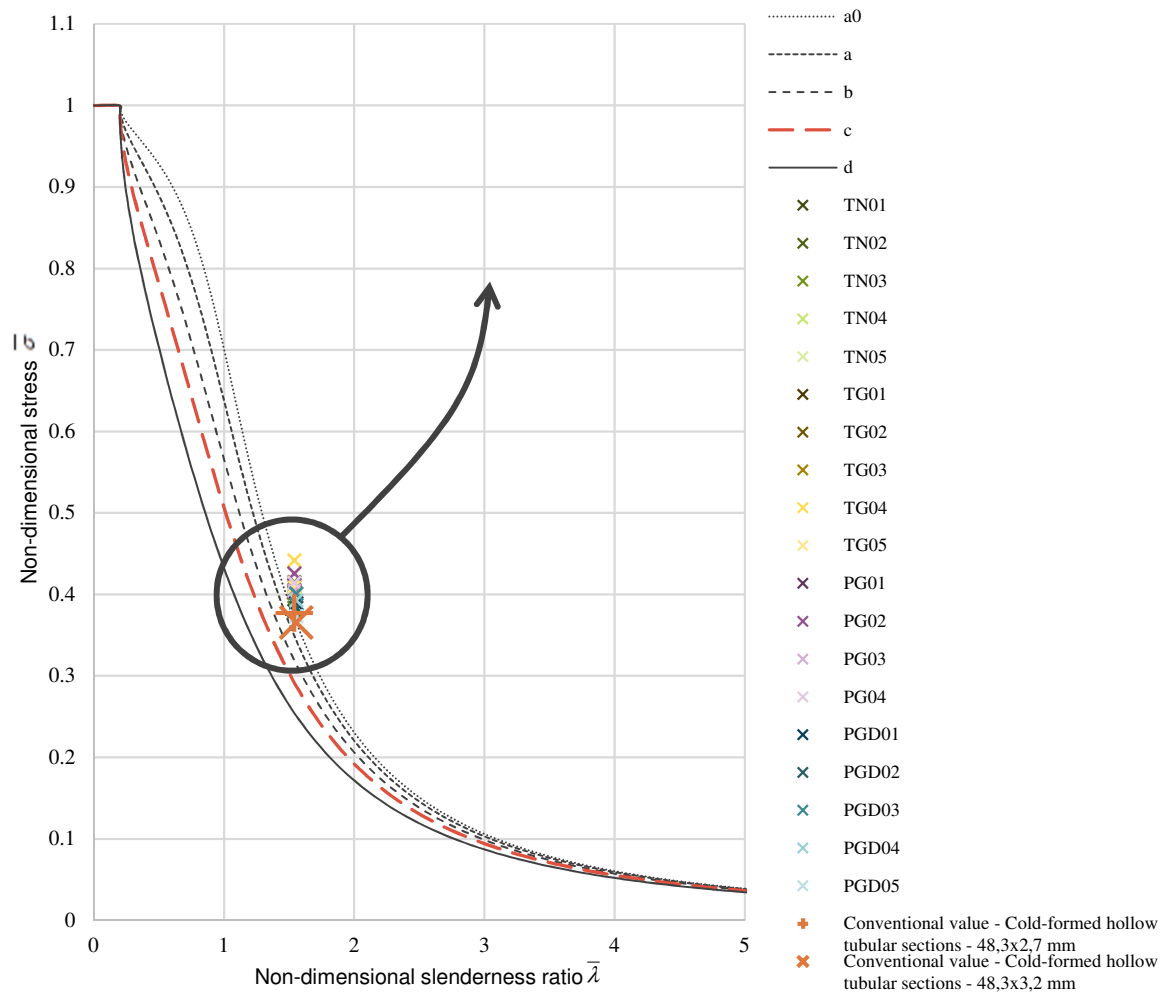


Figure 14 Comparison between experimental values and European buckling curves for cold-formed elements

From the equation of the European buckling curves (equation (17)), drawn up by Maquoi and Rondal [29], the values of imperfection factor α stemming from the experimental were determined (Table 8).

Table 8 Experimental values of the imperfection factor for cold-formed simply supporter members

Section	α
48.3 x 3.2 mm	0.1312
48.3 x 2.7 mm	0.1147

It is apparent that the standard theoretical imperfection factor of Eurocode 3 is nowhere near the test results with respect to the cold-formed elements. The imperfection factor determined from the statistical study of the experimental test was less than 0.21; so closer to the imperfection factor of hot-rolled hollow tubular sections than the current imperfection factor of cold-formed ones.

These tests on simply supported members enable to assess initial imperfections of a single element. However, other initial imperfections may be present in a structure like inclinations between vertical components. Full-scale tests on scaffolding ladders were therefore carried out to determine the importance of this lack of fit at joints between scaffoldings standards and their influence on the buckling behaviour.

2.3.3 Calibrations of an analytical model and a finite element model

As before, these experimental results will be used to calibrate two models: the analytical model and the finite element model.

Since the test configuration has not changed compared to the hot-rolled element tests, the two models, analytical and finite element, are identical. Only the calibration of these models was distinct. Indeed, the aim was to determine the degree of imperfection to better reflect the force-deflection response of the cold-formed element tests.

As regards the analytical model, three imperfection factor values will be compared:

- (i) an imperfection factor of 0.49: the conventional value for this type of section established by Eurocode 3;
- (ii) an imperfection factor of 0.21: the imperfection factor value as close as possible to the values obtained by the statistical study;
- (iii) an imperfection factor value obtained through the calibration of the analytical model.

Figure 15 and Figure 16 compare finite element analysis results and analytical analysis results with the experimental load-deflection responses at mid-height of cold-formed simply supported elements.

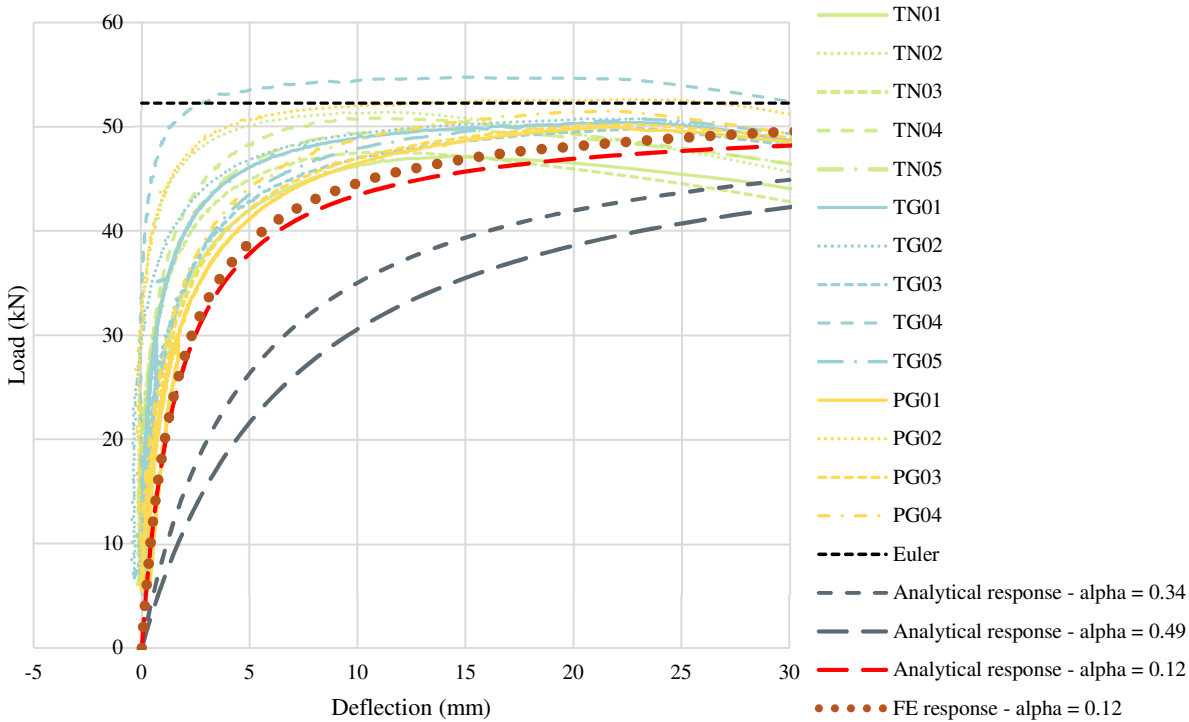


Figure 15 Calibration of load-deflection responses at mid-height of the 2.7 mm of thickness cold-formed elements

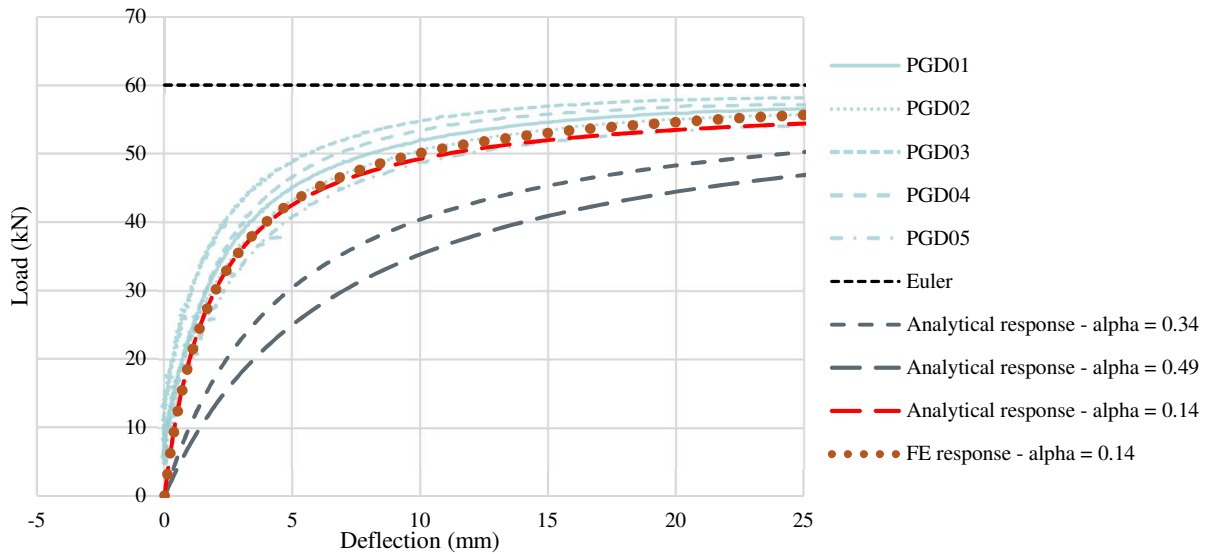


Figure 16 Calibration of load-deflection responses at mid-height of the 3.2 mm of thickness cold-formed elements

The calibration results show that an imperfection factor of 0.12 and 0.14, for 2.7 mm and 3.7 mm of thickness respectively, gives a load-deflection response similar to the experimental one. These two imperfection factor values, derived from the analytical and finite element models, are significantly close to the values derived from the statistical study of the experimental results. The comparison of the load-deflection responses obtained with the analytical model and the finite element model shows, once again, that these two models are equivalent. The both accurately predict the behaviour and failure load of cold-formed simply supported members.

The comparison of the analytical response with an imperfection factor of 0.49 to the experimental results makes it possible to affirm this response does not reflect the real behaviour of the structure. This implies that the initial imperfection degree of a buckling curve ‘c’, i.e. an imperfection factor of 0.49, is too important. The initial imperfections affecting these elements are actually considerably slighter, as experimentation has shown. An imperfection factor of 0.21, i.e. a buckling curve ‘a’, would make it possible to get closer to the experimental response while nevertheless preserving a safety margin as shown by Khamisi [26] in his thesis dissertation.

3 Experimental tests on scaffolding ladders

3.1 Experimental procedure

The second step of the test campaign launched in the laboratory consists of carrying out tests on scaffolding ladders (Figure 17) [30]. The test device (Figure 18) enabled to test ladders of 4 meters high and 0.7 meters wide, under axial compression. A total of nine elements was tested.

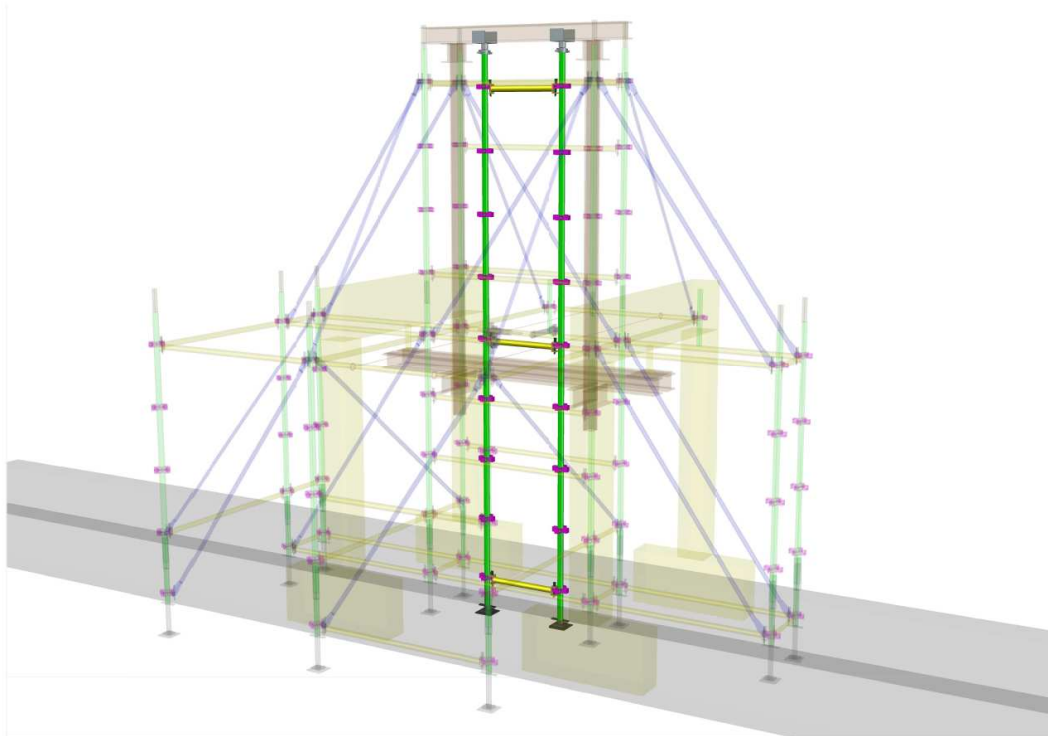


Figure 17 The testing element: scaffolding ladder

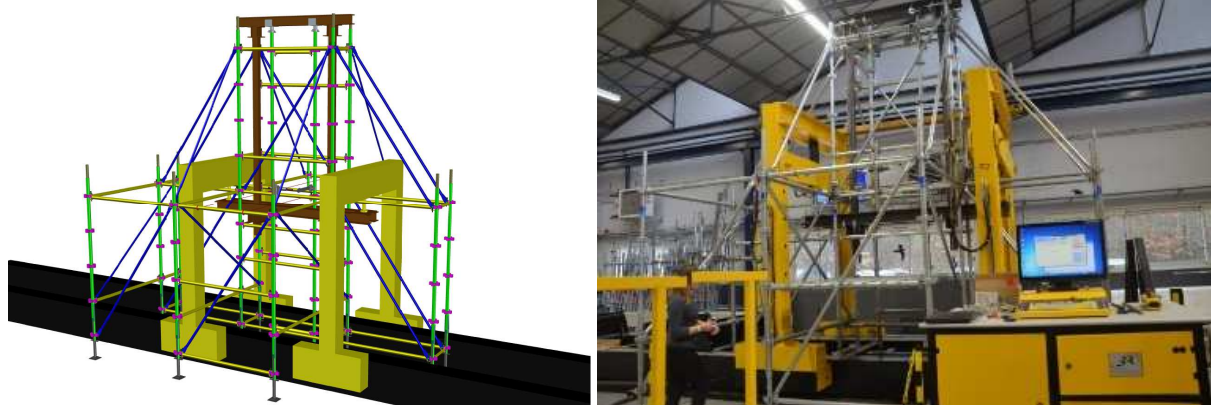


Figure 18 Full-scale test device for scaffold ladders

An appended structure was created to ensure the assembly and restrain out-of-plane displacement of the tested structures as illustrated in Figure 19a. No load was applied on this appended structure. The testing device consists on a trimmer to transmit the load between the loading frame and the top of the structure tested (Figure 19b), and a wire rope to restrain its out-of-plane displacements (Figure 19c). The scaffolding ladders were tested under pure compression. The loads were applied by hydraulic cylinders located on the loading frames (Figure 19d) on the trimmer to transmit the load to the top of the ladder.

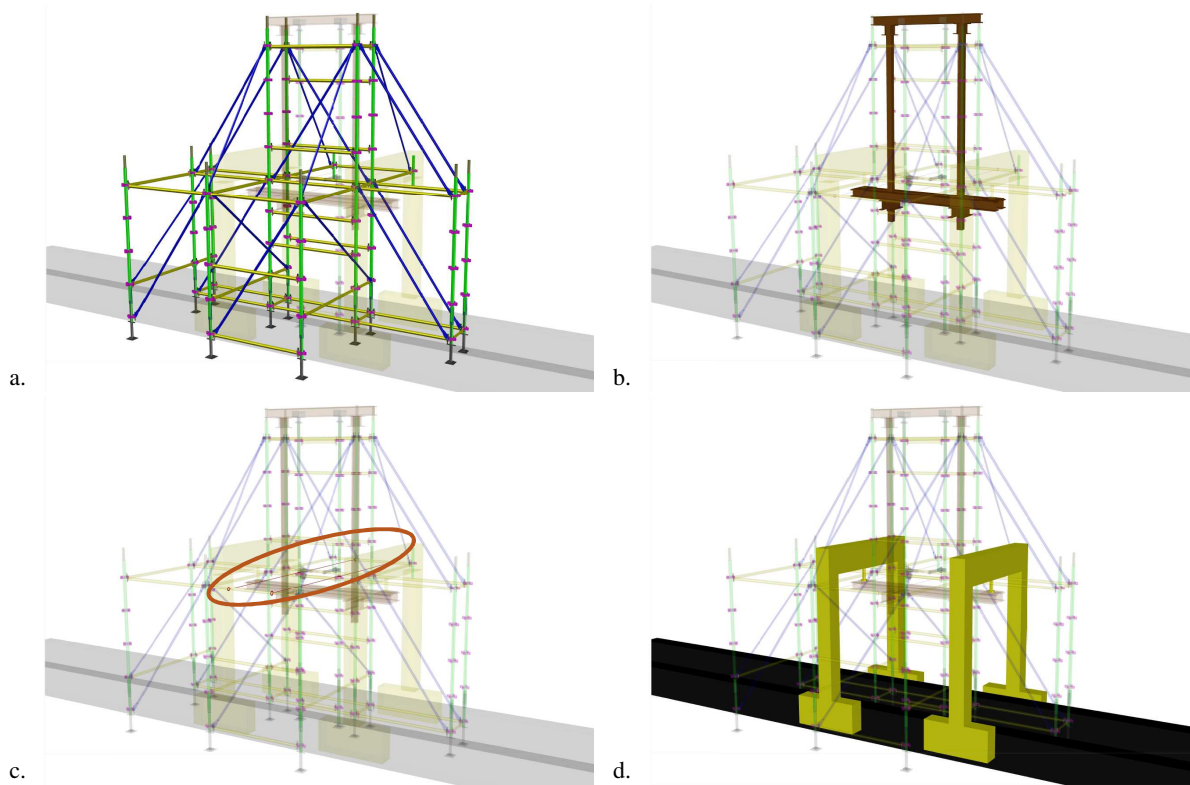


Figure 19 a) Appended structure; b) Trimmer; c) Wire rope; d) Loading frames

The ladders were tested in two support configurations: (i) screwdriver's supports (Figure 20a) to behave like the pin-jointed supports; (ii) clevises and screw jack feet (Figure 20b) to act as the real supports of scaffolding structures (stiffness: 20 kN.m/rad).

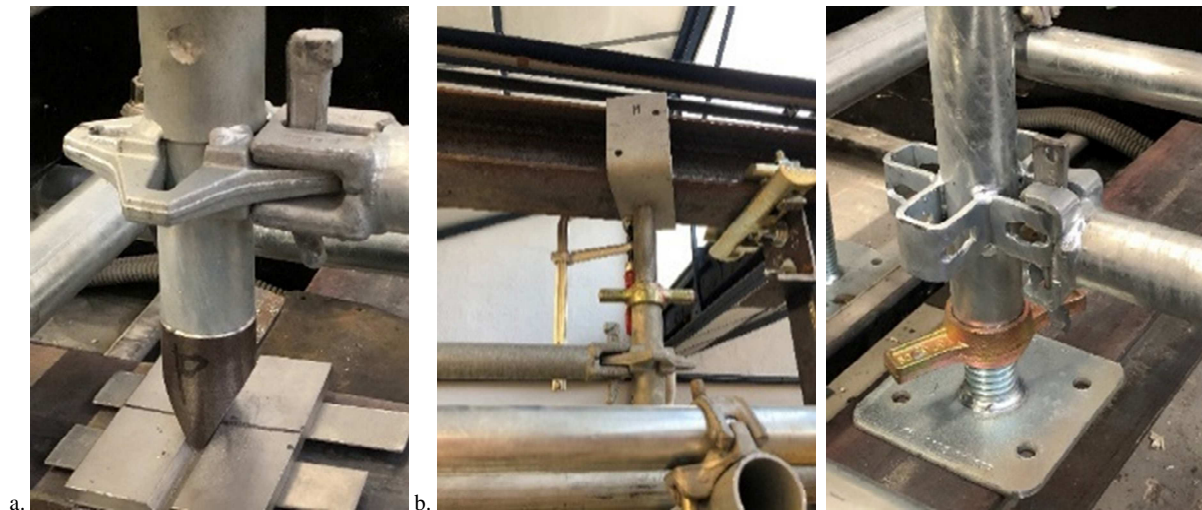


Figure 20 a) Screwdriver supports; b) Clevises and screw jack feet

The test was carried out with materials from several scaffolding suppliers. The cross-sectional characteristics of these scaffoldings are presented in Table 9. All the cross-sections were cold-formed hollow tubular sections.

Table 9 Properties of cross-sections of the scaffolding ladders

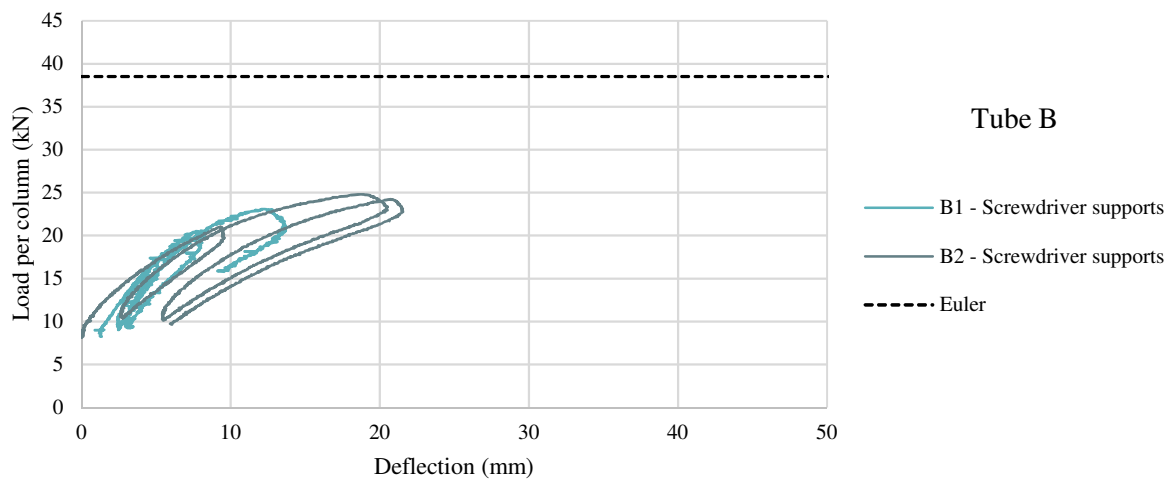
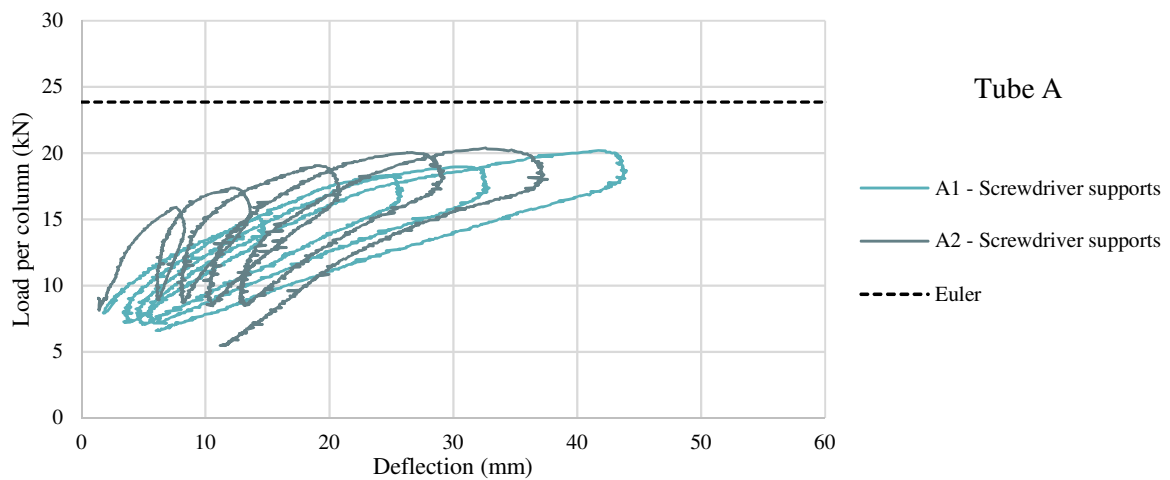
Section	Yield strength (MPa)	Stiffness between standard and transom (kN.m/rad)

Tube A	48.3x2.7 mmm	320	22
Tube B	48.3x2.9 mmm	320	83
Tube C	48.3x2.9 mmm	460	111

The horizontal deflections of the ladders were measured halfway up, i.e. 2 meters from the case level, using a displacement sensor. This sensor was connected to a central processing unit to acquire the data and monitor the deflection of the ladder according to the load applied by both loading frames. Several loading and unloading cycles were performed. The experimental load-deflection responses were therefore obtained.

3.2 Test results

Figure 21 and Figure 22 illustrate the experimental load-deflection responses obtained from the acquisition of the measurements at mid-height of the scaffolding ladders.



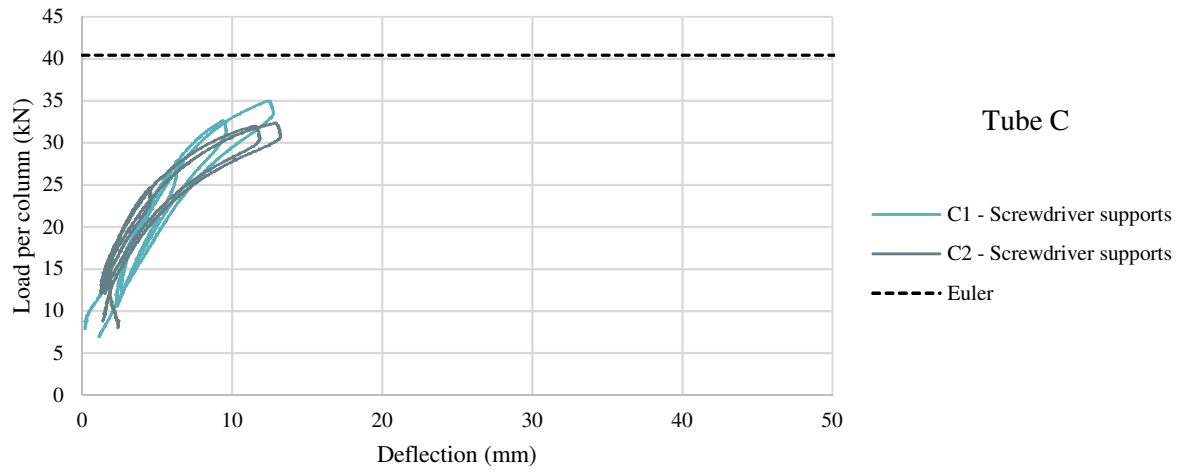
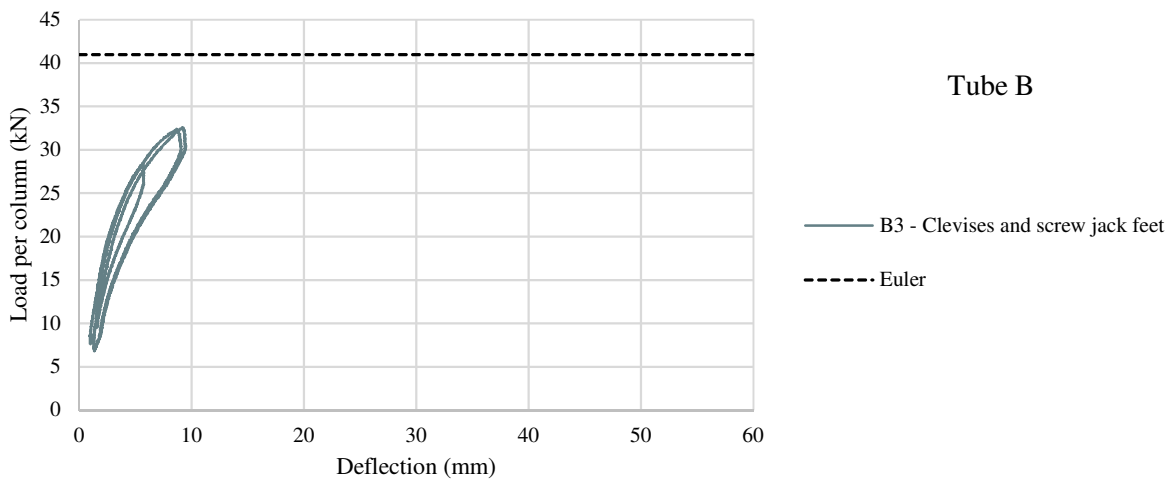
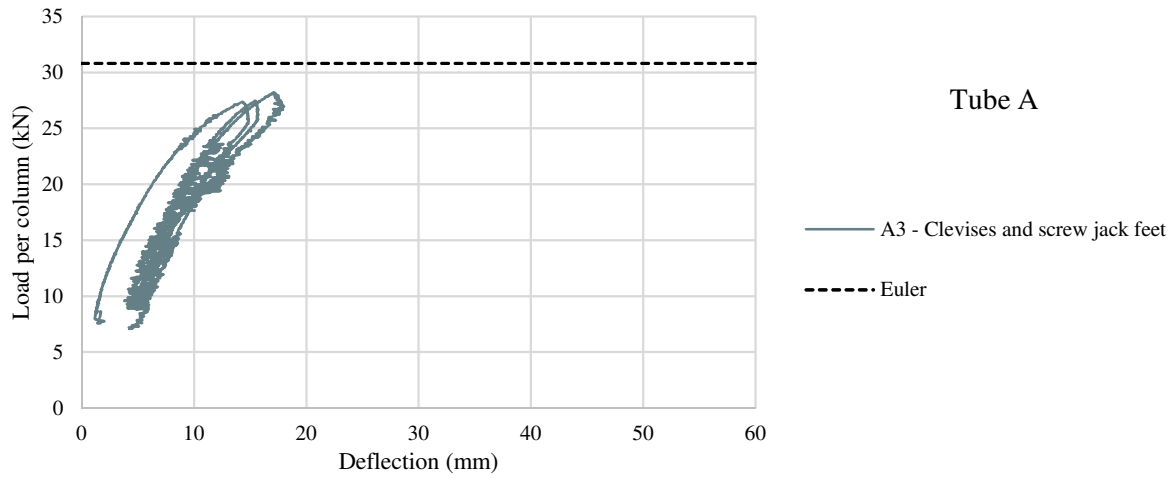


Figure 21 Experimental load-deflection responses at mid-height of the scaffolding ladders with screwdriver supports



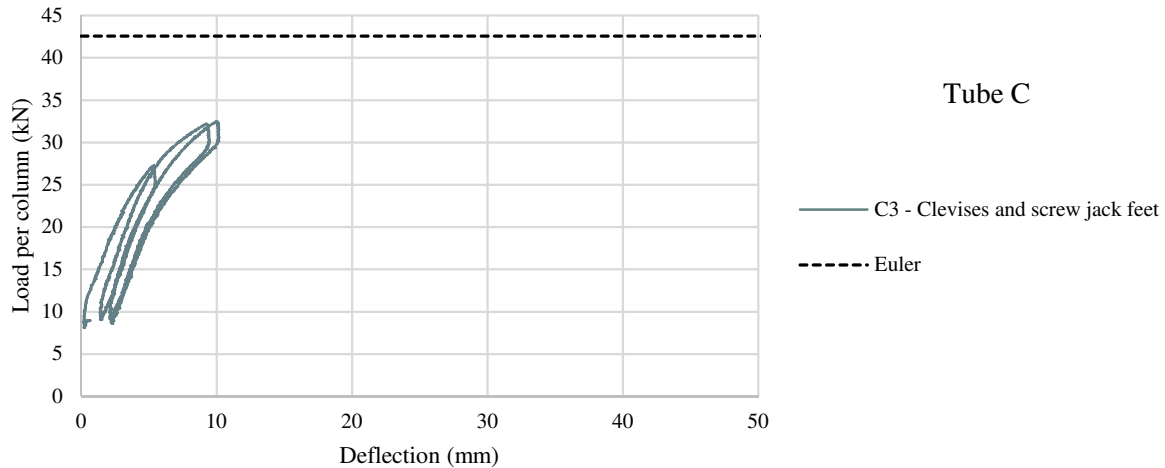


Figure 22 Experimental load-deflection responses at mid-height of the scaffolding ladders with clevises and screw jack feet

Loosenesses were observed during the first two loading cycles. These loosenesses were due to the assembly clearances of the vertical components with each other (inclinations between vertical components). The maximal assembly clearances, i.e. the play between the nominal inner diameter of the tube and the nominal outer diameter of the spigot, measured on the tested ladders did not exceed 3 mm.

Table 10 presents the failure load of each scaffolding ladder tested. These ultimate loads were obtained after several loading cycles.

Table 10 Experimental failure load of scaffolding ladders (in kN)

	Tube A	Tube B	Tube C
1	21.22	33.37	37.66
2	21.88	33.57	37.52
3	28.18	37.9	40.40

3.3 Statistical study

The statistical study is conducted on the similar principle as the two previous ones. The tests on the scaffolding ladders being expensive, only one or two tests were carried out for each configuration. The statistical study was therefore unconduted on the values of failure stresses but on the values of imperfection factors resulting from the experimentation.

The imperfection factors stemming from the experimentation were determined from the equation of European buckling curve of Maquoi and Rondal [29] and are given in the Table 11.

Table 11 Experimental imperfection factor of scaffolding ladders

	Tube A	Tube B	Tube C
1	0.235	0.215	0.128
2	0.170	0.205	0.135
3	0.145	0.105	0.090

Figure 18 allows the comparison between the experimental results and European buckling curves. The buckling curve ‘c’, relating to the cold-formed sections, is emphasised.

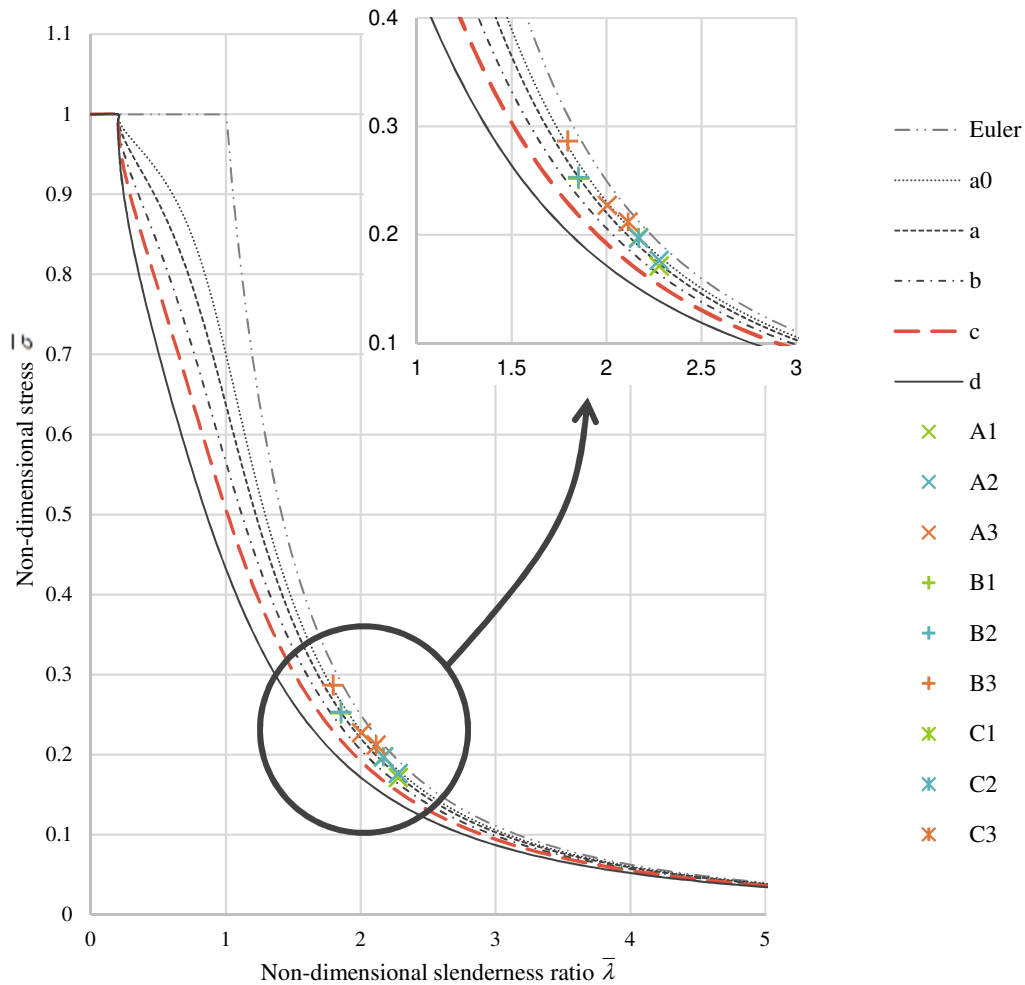


Figure 12 Comparison between experimental values and European buckling curves for scaffolding ladders

The values of V_1 and V_2 , given by Table 12, show that the distribution of the results of scaffolding ladder tests can be considered as normal distribution.

Table 12 Parameters of the method of the moments for tests on scaffolding ladders

N	m	s	V_1	V_2
9	0.1587	0.047	0.278	2.988

The convention value of the imperfection factor is therefore done by the equation:

$$\alpha = m + 2s \quad (21)$$

The convention value of the imperfection factor for scaffolding ladder tests is: $\alpha = 0.252$.

Figure 23 plots the distribution of experimental results. The conventional value of the imperfection factor is emphasised. It can be observed that the totality of the experimental results obtained is below the conventional imperfection factor resulting from the statistical study. Eurocode [28] states the 95% fractile value as the characteristic value, for an unfavourable high value. The conventional imperfection factor value are therefore safe.

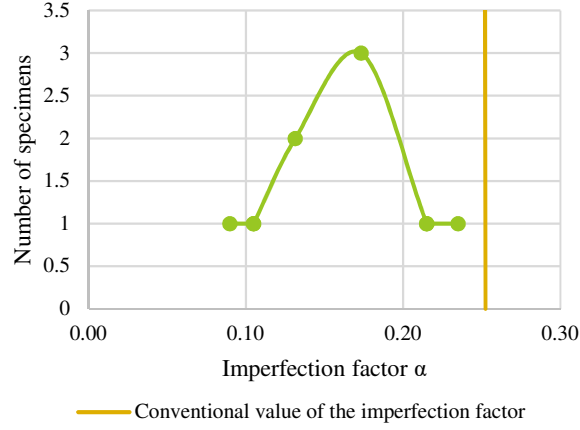


Figure 23 Distribution of experimental results for scaffolding ladders

The results of these full-scale tests highlight that the conventional imperfection factor for cold-formed hollow tubular sections, i.e. $\alpha = 0.49$, is too safe and too constraining as regard of the sections used in the field of scaffolding. Based on these results, it is possible to admit an imperfection factor of 0.34 would allow a better estimation of the initial imperfections affecting this type of element while nevertheless preserving a safety margin.

3.4 Calibrations of an analytical model and a finite element model

As for simply supported members, the experimental load-deflection responses will be used to calibrate two models: an analytical model and a finite element model.

For the analytical model, the mid-height deflection of the column must be expressed as a function of the load applied to the column. The deflection Δ physically measured at mid-height of the ladder is:

$$\Delta = d_{fin} - d_0 = d_0 \cdot \frac{N}{N_{cr} - N} \quad (22)$$

where: d_{fin} is the total displacement under axial load, d_0 is the initial imperfection of the scaffolding ladder, N is the compression load and N_{cr} is the critical load.

The initial displacement d_0 is given by the expression below:

$$d_0 = e_0 + e_{0,sup} = e_0 \cdot \left(1 + \sin \left(\frac{\pi \cdot h_{e_{0,sup}}}{L_{cr}} \right) \right) \quad (23)$$

where $e_{0,sup}$ is the initial imperfection determined on the height $h_{e_{0,sup}}$, $h_{e_{0,sup}}$ represents the distance between the upper inflection point and the top of the scaffolding ladder (Figure 24) and e_0 is the initial imperfection defined in the article 5.3.2 (11) of Eurocode 3 Part1-1 as:

$$e_0 = \alpha \cdot (\bar{\lambda} - 0,2) \cdot \frac{W_{el}}{A} \quad (24)$$

The critical load is obtained from the equation:

$$N_{cr} = \frac{\pi^2 EI}{L_{cr}^2} \quad (25)$$

where L_{cr} is the buckling length of the element. The tested elements were scaffolding ladders; the buckling length does not equal the length of the elements. Under axial compression, the scaffolding ladder was deformed as shown in Figure 24. The buckling length represents the length between two

consecutive turning points. The buckling length of each configuration tested is summarized in Table 13.

Table 13 Buckling length L_{cr} of the scaffolding ladders (in meter)

	Screwdriver supports	Clevises and screw jack feet
Tube A	2.961	2.605
Tube B	2.340	2.326
Tube C	2.342	2.282

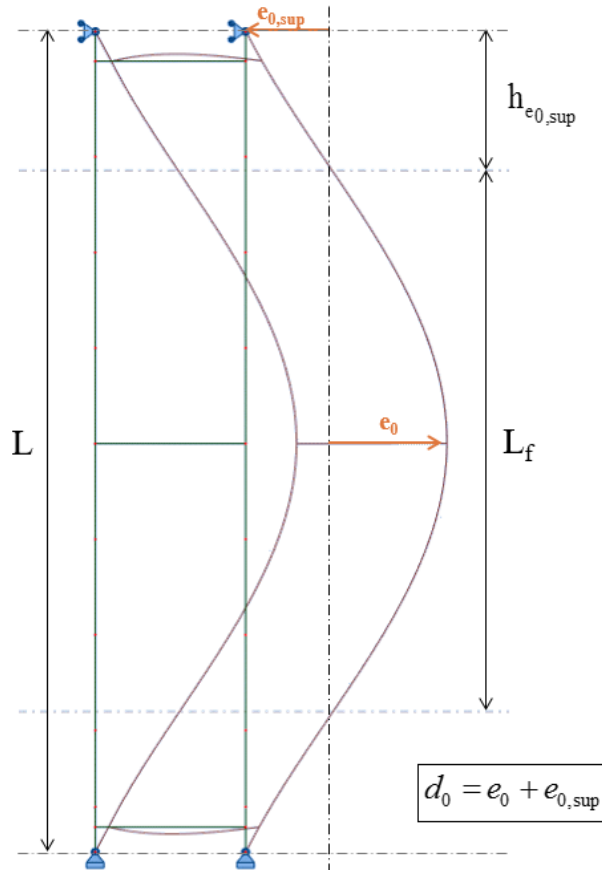


Figure 24 Deformation of the scaffolding ladder under axial load

Equations (26) to (27) hence make it possible to establish the load-deflection response of a scaffolding ladder for any value of imperfection factor α , i.e. several amplitudes of initial imperfections. It will thus be possible to compare the experimental response to different analytical responses, to obtain the analytical model that best reflects the actual behaviour of the structure. Three imperfection factor values will be compared:

- (i) an imperfection factor of 0.49: the conventional value for this type of cross-section established by Eurocode 3;
- (ii) an imperfection factor of 0.34: the imperfection factor value as close as possible to the values obtained by the statistical study;
- (iii) an imperfection factor value obtained through the calibration of the analytical model.

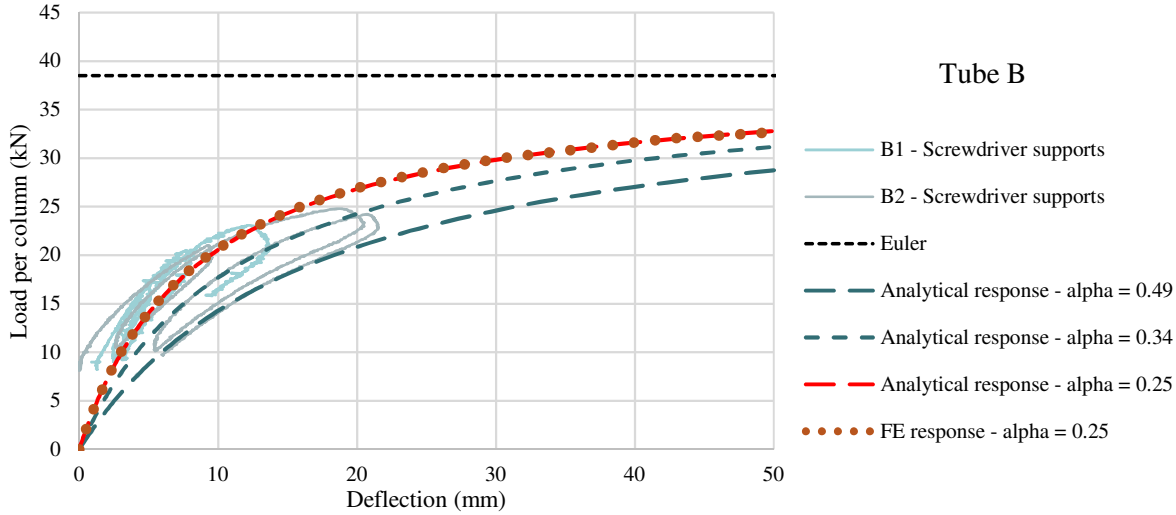
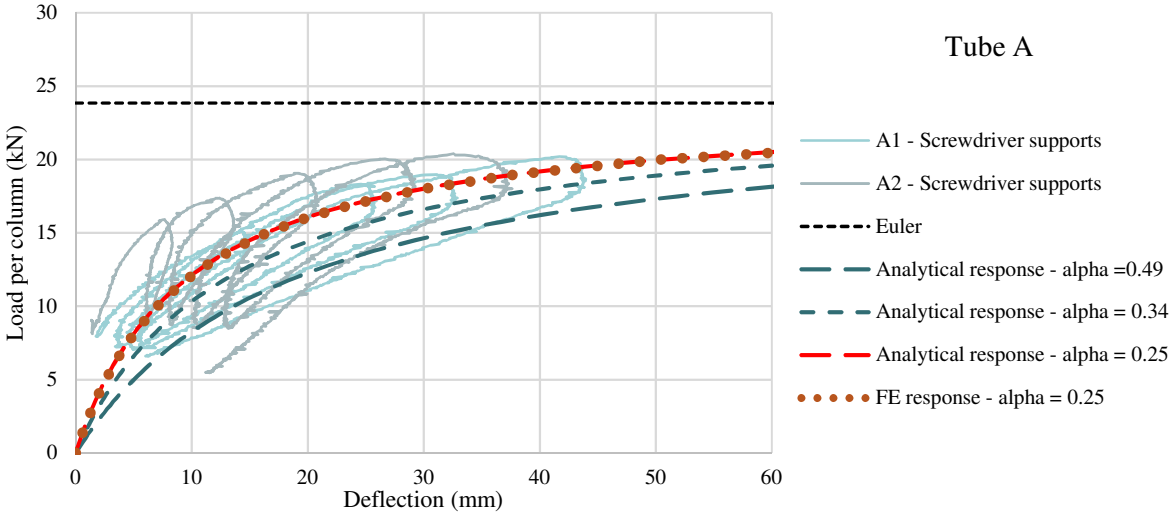
The second model developed is a finite element model. The software suite for finite element analysis Abaqus was used to create this finite element model. The measured dimensions of the components were used for cross-sectional properties in the finite element models. The nonlinearity properties of the steel material are applied to the model. The stress-strain relationship is based on results of tensile tests

carried out on specimens from tested hot-rolled elements.

The standard/transom stiffness, given in Table 9, has been taken into account in all models. The ladders with screwdriver supports were modelled with pin-jointed supports; while the ladders with clevises and screw jack feet were modelled with supports with a stiffness of 20 kN.m/rad.

The calibration was achieved by changing the amplitude of the initial imperfections of the model, to obtain the finite element model that best reflects the actual behaviour of the structure. The failure (ultimate load) in the finite element model was observed when the load limit point was reached, which was associated with significant displacements.

Figure 25 and Figure 26 compare finite element analysis results and analytical analysis results with the experimental load-deflection responses at mid-height of hot-rolled simply supported elements.



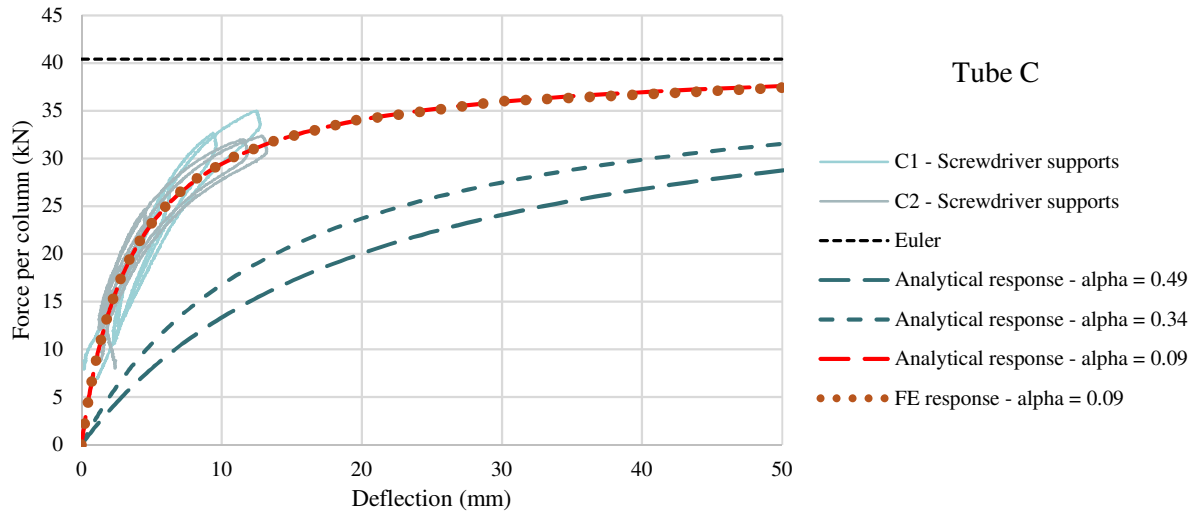
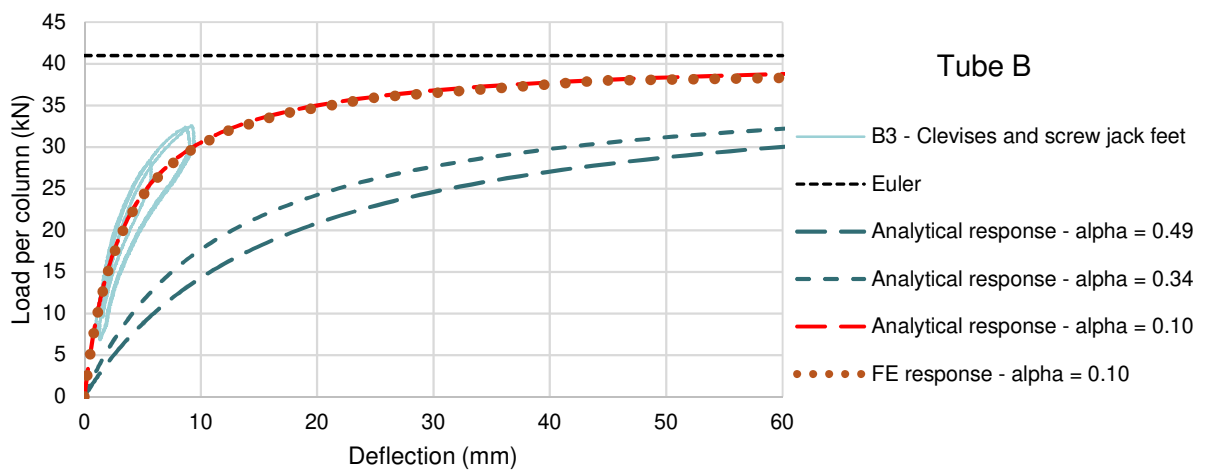
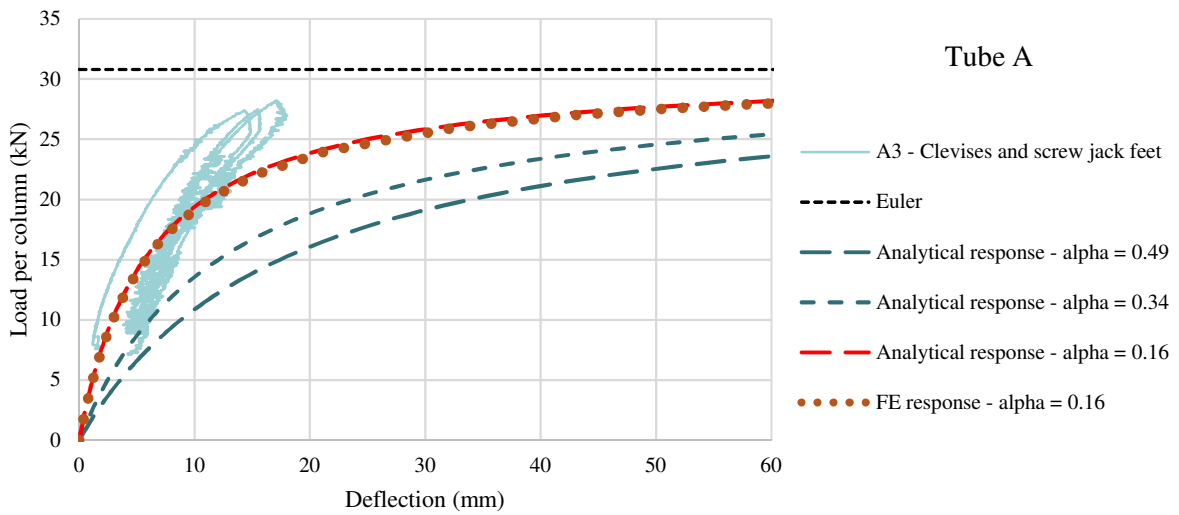


Figure 25 Calibration of load-deflection responses at mid-height of the scaffolding ladders with screwdriver supports



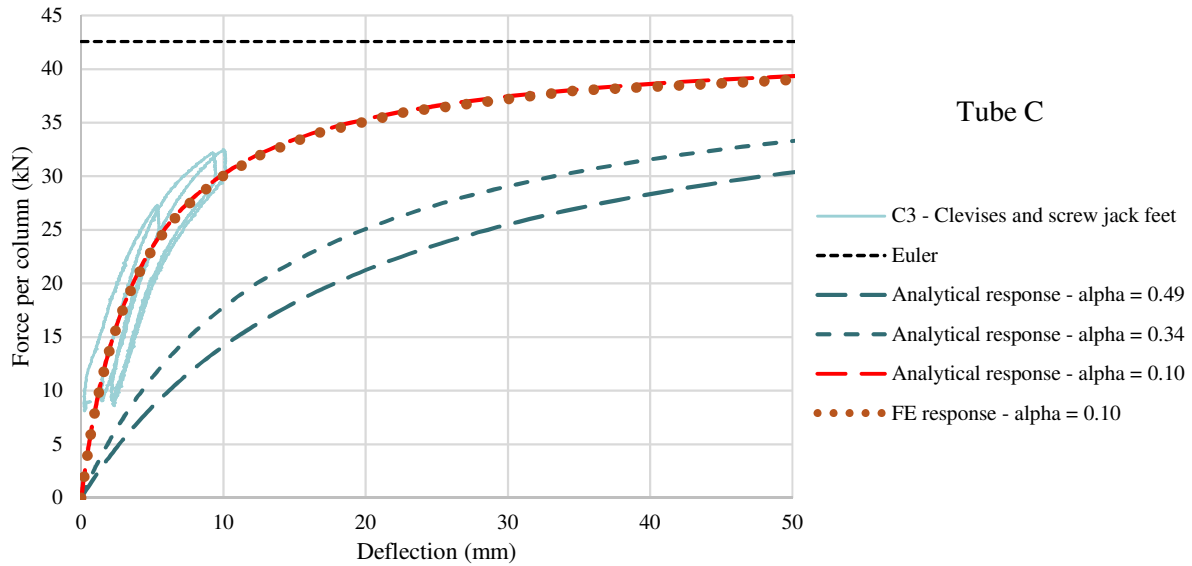


Figure 26 Calibration of load-deflection responses at mid-height of the scaffolding ladders with screw jack feet

The calibration of analytical and finite element models shows that the imperfection factor must be lower or at most equal to 0.25 to obtain a load-deflection response similar to the experimental one. The imperfection factor values obtained above are considerably lower than the conventional value of 0.49 imposed by Eurocode 3 for this type of cross-section. Moreover, when comparing the analytical response with an imperfection factor of 0.49 with the experimental responses, it can be noted that this response does not reflect the actual behaviour of scaffolding ladders. This implies that the initial imperfection degree of a buckling curve ‘c’, i.e. an imperfection factor of 0.49, is too important.

It can equally be sighted that the imperfection values resulting from analytical and finite element model are close to or even lower than the value of 0.252 resulting from the statistical study. This implies this value of 0.252 is well representative of the behaviour of this type of structure while being safe.

The comparison of the load-deflection responses obtained with the analytical model and the finite element model shows once again that these two models are equivalent and both accurately predicting the behaviour and failure load of scaffolding ladders.

The observation of the previous results makes it possible to affirm that an imperfection factor of 0.34, i.e. a buckling curve ‘b’, would make it possible to get closer to the real behaviour of this type of element while nevertheless preserving a safety margin.

4 Conclusion

A series of experimental tests were conducted to determine and analyse the buckling behaviour of scaffolding structures. These tests were carried out on the one hand on simply supported members, hot-rolled or cold-formed, and on the other hand on scaffolding ladders, which govern the entire behaviour of an entire scaffolding structure.

The experimentation revealed that for all the elements tested, the intensity of the initial imperfection required by the Eurocode 3 standard, through the buckling curves, were far too important. However, it is pertinent to remember that if the initial imperfections of a structure are overestimated, this leads to an overestimation of the evaluation of the internal stresses and therefore, *in fine*, to the oversizing of the structure. It is therefore crucial for all designers of scaffolding structures to have an accurate estimate of the initial imperfections affecting their structures to be able to design them optimally. Accurate estimation of initial imperfections leads to optimal designing.

It was therefore shown in this article that the behaviour of the hot-rolled elements was closer to the buckling curve 'a₀', i.e. a 0.13 imperfection factor, than to the buckling curve 'a', i.e. a 0.21 imperfection factor, as currently established in Eurocode 3. This result is applicable to elements whose diameter and slenderness range are those commonly found in the scaffold field.

Similarly, the tests on simply supported cold-formed elements and on scaffolding ladders highlighted that the standard theoretical buckling behaviour of these sections (buckling curve 'c', i.e. a 0.49 imperfection factor), established by Eurocode 3, does not reflect their actual behaviour and is too restrictive.

The tests on simply supported cold-formed members provided an experimental imperfection factor of 0.12. These tests enabled to assess the initial imperfections that affect only one element, i.e. geometrical imperfections and residual stresses.

For this reason, the tests on scaffolding ladders were conducted. Indeed, in the case of tests on scaffolding ladders, the initial imperfections measured are equally the geometrical imperfections and residual stresses of each constituent element but also the set of imperfections affecting the structure as a whole, i.e. any inclinations between vertical components. In this case the experimentation has shown that the initial imperfections affecting these structures lead to an imperfection factor of 0.25. This value of 0.25 is the result of tests on scaffolding ladders and therefore takes into account the lack of fit at joints between scaffolding standards, within the assembly clearance limit of 3mm (maximum value observed during tests). This play of 3 mm is ordinary for scaffolding elements. Nevertheless, for a more significant clearance between tubular standards and spigots, it would be necessary to model this inclination between vertical components, in accordance with the EN 12811-1 standard [31], in addition to the initial imperfection advocated in this article.

To get closer to the buckling curves currently defined in Eurocode 3, it is therefore proposed to adopt an imperfection factor of 0.34 to represent the behaviour of scaffolding structures. This value of 0.34 applies for cold-formed steel circular hollow tubular sections with a slenderness ratio between 1.5 and 2.5, a cross-sectional area common in scaffolding and with assembly clearances not exceeding three millimetres. On the materials investigated, this valuation of the buckling curve (from curve 'c' to curve 'b') allows a resistance gain of 5% on average. Further studies required needed for a more universal application of the value of 0.34.

Two models have equally been developed through this article: an analytical model and a finite element one. The comparison of load-deflection responses show that these both models provide reasonable agreement compared to the experimental responses. As a result, these two models combined with the imperfection factor of 0.34 make it possible to accurately predict the behaviour and failure load of scaffolding ladders. This value can then be used for the design of scaffolding structures [23,30].

References

- [1] ECS. NF EN 1993-1-1: Eurocode 3: Design of steel structures. Part 1-1: General rules and rules for buildings 2005.
- [2] Sfintesco D. Fondement expérimental des courbes européennes de flambement. *Construction Métallique* 1970;3:5–12.
- [3] Milojkovic B. Factors of safety for standard scaffold structures. Doctoral thesis. Oxford Brookes University, 1999.
- [4] Milojkovic B, Beale RG, Godley MHR. - Determination of the factors of safety of standard scaffold structures. In: Chan SL, Teng JG, Chung KF, editors. *Advances in Steel Structures (ICASS '02)*, Oxford: Elsevier; 2002, p. 303–10. <https://doi.org/10.1016/B978-008044017-0/50035-4>.
- [5] Pallet PF, Burrow MPN, Clark LA, Ward RT. Investigation into aspects of falsework. vol. Contract Research Report 394/2001. 2001.

- [6] Lew HS. CONSTRUCTION FAILURES AND THEIR LESSONS. *Null* 1984;12:272–5. <https://doi.org/10.1080/09613218408545283>.
- [7] Peng JL, Wang CS, Lin CC, Lin SK. Stability of independent heavy-duty scaffolds: an experimental study. *Advanced Steel Construction* 2017;13:318–42. <https://doi.org/10.18057/IJASC.2017.13.4.1>.
- [8] Chandrangsu T, Rasmussen KJR. Structural modelling of support scaffold systems. *Journal of Constructional Steel Research* 2011;67:866–75. <https://doi.org/10.1016/j.jcsr.2010.12.007>.
- [9] Chandrangsu T, Rasmussen KJR. Structural modelling of support scaffold systems. The University of Sydney; 2009.
- [10] Peng JL, Pan ADE, Chan SL. Simplified models for analysis and design of modular falsework. *Journal of Constructional Steel Research* 1998;48:189–209. [https://doi.org/10.1016/S0143-974X\(98\)00198-9](https://doi.org/10.1016/S0143-974X(98)00198-9).
- [11] Peng JL, Pan AD, Rosowsky DV, Chen WF, Yen T, Chan SL. High clearance scaffold systems during construction —I. Structural modelling and modes of failure. *Engineering Structures* 1996;18:247–57. [https://doi.org/10.1016/0141-0296\(95\)00144-1](https://doi.org/10.1016/0141-0296(95)00144-1).
- [12] Peng J. L., Pan A. D. E., Chen W. F., Yen T., Chan S. L. Structural modeling and analysis of modular falsework systems. *Journal of Structural Engineering* 1997;123:1245–51. [https://doi.org/10.1061/\(ASCE\)0733-9445\(1997\)123:9\(1245\)](https://doi.org/10.1061/(ASCE)0733-9445(1997)123:9(1245)).
- [13] Cimellaro GP, Domaneschi M. Stability analysis of different types of steel scaffolds. *Engineering Structures* 2017;152:535–48. <https://doi.org/10.1016/j.engstruct.2017.07.091>.
- [14] Weesner LB, Jones HL. Experimental and analytical capacity of frame scaffolding. *Engineering Structures* 2001;23:592–9. [https://doi.org/10.1016/S0141-0296\(00\)00087-0](https://doi.org/10.1016/S0141-0296(00)00087-0).
- [15] Peng J-L, Wu C-W, Chan S-L, Huang C-H. Experimental and numerical studies of practical system scaffolds. *Journal of Constructional Steel Research* 2013;91:64–75. <https://doi.org/10.1016/j.jcsr.2013.07.028>.
- [16] Klasson A, Crocetti R, Hansson EF. Slender steel columns: How they are affected by imperfections and bracing stiffness. *Structures* 2016;8:35–43. <https://doi.org/10.1016/j.istruc.2016.08.004>.
- [17] Cai J, Liu Y, Feng J, Tu Y. Nonlinear stability analysis of a radially retractable suspen-dome. *Advanced Steel Construction* 2017;13:117–31. <https://doi.org/10.18057/IJASC.2017.13.2>.
- [18] Gao L, Jiang K, Bai L, Wang Q. Experimental study on stability of high strength steel long columns with box-sections. *Advanced Steel Construction* 2017;13:339–411. <https://doi.org/10.18057/IJASC.2017.13.4.5>.
- [19] Iu C-K. Generalised element load method with whole domain accuracy for reliable structural design. *Advanced Steel Construction* 2016;12:466–86. <https://doi.org/10.18057/IJASC.2016.12.4>.
- [20] Chan JL., Lo SH. Stability design of system scaffold with differential settlement. *Structures* 2020;27:1467–78. <https://doi.org/10.1016/j.struct.2020.07.024>.
- [21] Liu SW, Chan JLY, Bai R, Chan SL. Curved-quartic-function elements with end-springs in series for direct analysis of steel frames. *Steel and Composite Structures* 2018;29:623–33. <https://doi.org/10.12989/scs.2018.28.5.623>.
- [22] Mercier C, Khelil A, Khamisi A, Al Mahmoud F, Boissiere R, Pamies A. Analysis of the global and local imperfection of structural members and frames. *Journal of Civil Engineering and Management* 2019;25:805–18. <https://doi.org/10.3846/jcem.2019.10434>.
- [23] Mercier C, Khelil A, Al Mahmoud F, Khamisi A, Boissiere R, Blin-Lacroix J-L, et al. Lateral stability of slender cold-rolled hollow tubular sections with initial imperfections. *Engineering Structures* 2020;219:110840. <https://doi.org/10.1016/j.engstruct.2020.110840>.
- [24] Yang L, Zhao M, Chan T, Shang F. Flexural buckling design of fabricated austenitic and duplex

stainless steel columns. *Advanced Steel Construction* 2018;14:184–205. <https://doi.org/10.18057/IJASC.2018.14.2.4>.

- [25] Zhao Z, Chen Z. Analysis of door-type modular steel scaffolds based on a novel numerical method. *Advanced Steel Construction* 2016;12:316–27. <https://doi.org/10.18057/IJASC.2016.12.3.6>.
- [26] Khamisi A. Stability of tubular steel structures: buckling and lateral torsional buckling. University of Lorraine, 2016.
- [27] Jacquet J. Essais de flambement et exploitation statistique. *Construction Métallique* 1970;3:13–36.
- [28] CEN. NF EN 1990: Eurocode: Basis of structural design 2003.
- [29] Maquoi R, Rondal J. Mise en équation des nouvelles courbes européennes de flambement. *Construction Métallique* 1978;1:17–30.
- [30] Mercier C. Development of a model of stability for steel hollow tubular section beam-columns sensitive to second order effects. University of Lorraine, 2019.
- [31] ECS. NF EN 12811-1: Temporary works equipment. Part 1: Scaffolds - Performance requirements and general design 2004.